

Organic Superconductors: when correlations and magnetism walk in

Denis Jérôme

Received: date / Accepted: date

Abstract This survey provides a brief account for the start of organic superconductivity motivated by the quest for high T_c superconductors and its development since the eighties'. Besides superconductivity found in 1D organics in 1980, progresses in this field of research have contributed to better understand the physics of low dimensional conductors highlighted by the wealth of new remarkable properties. Correlations conspire to govern the low temperature properties of the metallic phase. The contribution of antiferromagnetic fluctuations to the interchain Cooper pairing proposed by the theory is borne out by experimental investigations and supports superconductivity emerging from a non Fermi liquid background. Quasi one dimensional organic superconductors can therefore be considered as simple prototype systems for the more complex high T_c materials.

Keywords Superconductivity · Organic superconductors · One dimensional conductors

PACS 74.70.Kn, 74.25.F, 74.62.-c

1 Superconductivity in the seventies

Bardeen, Cooper and Schrieffer (BCS)[1] had emphasized in 1957 the existence of a two body attractive interaction between charge carriers (either electrons or holes) being a prerequisite for a Bose condensation of electron pairs into the superconducting state. This net attractive coupling in spite of the Coulomb repulsion between carriers of the same sign relies closely on an attraction between electrons mediated by their interaction with excitations of the lattice

D. Jérôme
Laboratoire de Physique des Solides, Université Paris-Sud, 91405 Orsay, France
Tel.: +(33)169155301
E-mail: denis.jerome@u-psud.f

namely, the phonons. In addition, a major achievement of the BCS theory has been the understanding of the ionic mass dependence of the critical temperature i.e. ($T_c \propto M^{-1/2}$). Although Fröhlich had proposed in 1954 a model for superconductivity based on the involvement of the lattice [2] this theory was unable to account for the superconductivity of metals but turned out to be quite relevant later for the interpretation of the transport properties in some one dimensional organic compounds, *vide infra*.

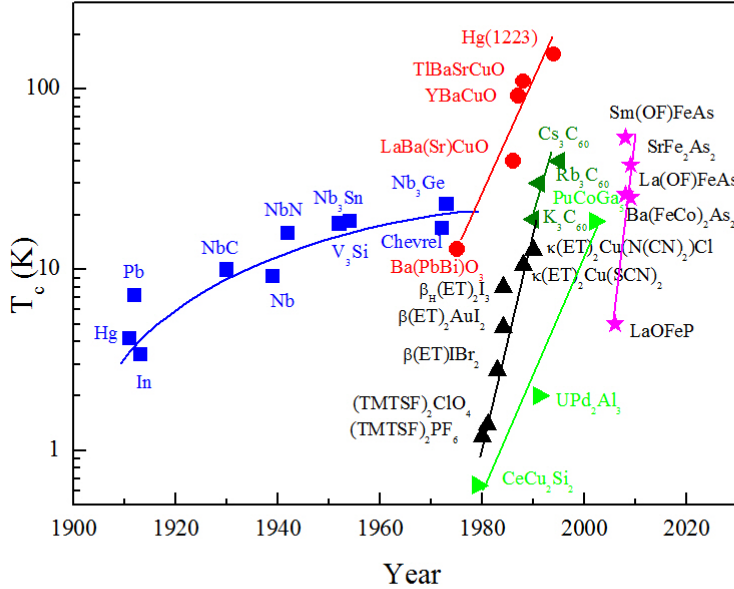


Fig. 1 Evolution of T_c in various series of superconductors over the years.

The search for new materials exhibiting increased critical temperatures T_c has been a strong motivation for research since the initial discovery of superconductivity by Kamerlingh Onnes[3] in 1911. The rise of T_c has been relatively slow during the first 50 years as shown on fig(1) with some kind of a saturation in the sixties.

At the beginning of the 60's the term *high temperature superconductor* was already commonly used referring to the intermetallic compounds of the A15 structure, namely, (Nb_3Sn or V_3Si)[4] see fig(1). These superconductors are still until now the materials used for building most superconducting magnets.

However, some new concepts for superconductivity had been recognized by Professor Friedel namely, the hidden 1D nature of the A15 structure which provides an enhancement of the density of states at the Fermi level lying close to the van-Hove singularity of the density of states. Within the BCS formalism large T_c could in turn be expected. They were actually observed (17-23 K) but an upper limit was found to the increase of T_c since the large value of $N(E_F)$

makes also the structure unstable against a cubic to tetragonal band Jahn-Teller distortion[5,6]. Labbé, Barišić and Friedel made the remark in 1967 that T_c 's of A15 compounds were not much influenced by the characteristic energy of the phonon spectrum but determined by the narrowness of the density of states at Fermi level. They also showed that the band filling of actual compounds such as Nb₃Sn and V₃Si makes their T_c 's optimum[7]. Consequently, based on metallurgical considerations, some authors at the end of the seventies considered 25-30 K, as an upper limit for T_c [8].

1.1 Some explorers

Although, at that time all attempts to increase T_c were still based on the BCS phonon-mediated theory with its strong coupling extension[9,10] some new paths were proposed.

A few years after the BCS paper, Kohn and Luttinger proposed a new mechanism for superconductivity[11] still based on the pairing idea although the attraction is no longer phonon-mediated. The attraction derives from an extension of Friedel's density oscillations around charged impurities in metals[12, 13]. This mechanism is an entirely electronic process. However, the expected critical temperature should be extremely small in the milli Kelvin range but Kohn and Luttinger emphasized that flat Fermi surfaces or van Hove singularities could greatly enhance the actual T_c .

Expanding the successful idea of the isotope effect in the BCS theory other models were proposed in which excitations of the lattice responsible for the electron pairing had been replaced by higher energy excitations namely, electronic excitations, with the hope of new materials with T_c higher than those explained by the BCS theory. Consequently, the small electronic mass m_e of the polarizable medium would lead to an enhancement of T_c of the order of $(M/m_e)^{1/2}$ times the value which is observed in a conventional superconductor, admittedly a huge factor. V.L.Ginzburg[14,15] considered in 1964 the possibility for the pairing of electrons in metal layers sandwiched between polarizable dielectrics through virtual excitations at high energy.

It is illuminating to have a look on fig(1) at the compound Ba(Pb_{0.8}Bi_{0.2})O₃ reported to become superconducting at 13 K[16]. This was in 1975 the highest T_c ever observed for an oxide. With this high temperature superconductivity in the perovskite series Ba(PbBi)O₃, *Déjà Napoléon pointait sous Bonaparte!* But, as Edelsack, Gubser and Wolf wrote in their introduction for the conference proceeding on Novel Superconductivity edited by Wolf and Kresin[17], *Organics were those who decided to forge revolutionary paths in the quest for high T_c .*

In this respect, W.A.Little had made an interesting suggestion in 1964[18, 19]: a new mechanism for superconductivity supposed to provide to a drastic enhancement of the superconducting T_c to be observed in especially designed macromolecules. The idea of Little was indeed strongly rooted in the extension of the isotope effect proposed by BCS.

However, a prerequisite to the model of Little was the achievement of conduction in molecular crystals namely, new types of conductors in which the conduction would proceed through the transport of charge between molecular orbitals rather than atomic orbitals.

Actually, the concept of a synthetic metal had already been launched by McCoy and Moore[20] when they proposed: *to prepare composite metallic substances from non-metallic constituent elements*. As to the possibility of superconductivity in materials other than metals, Fritz London in 1937[21] has been the first to suggest that compounds with aromatic rings such as anthracene, naphthalene,... *might exhibit a current running freely around the rings under a magnetic field*.

The first successful attempt to promote metal-like conduction between open shell molecular species came out in 1954 with the synthesis of the molecular salt of perylene oxidized with bromine [22] although this salt was rather unstable.

1.2 Organic metallicity

Coming back to 1D materials, the model of Little had not much in common with the early remark of London. It was based on the use of a long conjugated polymer such as a polyene molecule grafted by polarizable side groups[23]. Admittedly, this formidable task in synthetic chemistry has not reached its initial goal but the idea to link organic metallicity and one dimensionality was launched and turned out to be a very strong stimulant for the development of organic superconductors.

One dimensional conductors had been regarded previously as textbook examples by Peierls[24], who stated a theorem according to which a gap should spontaneously open at the Fermi level in the conduction and lead to the stabilization of a dielectric insulating state at low temperature ruining therefore any further hope for superconductivity. The point is that the seminal paper of Little[18] which was still based on the popular Fermi liquid BCS theory had made the assumption that the enhanced Cooper pair attraction would be strong enough to overcome the energy gain of a Peierls-distorted chain. Needless to say that a lot of basic problems namely, the possibility of synthesizing conducting polymer chains and the competition against a Peierls distortion, had been overlooked. Eighteen years later the Peierls transition has been established in platino-cyanate chains[25].

Bychkov *et-al*[26] criticized the model of Little regarding its potentiality to lead to high temperature superconductivity. Following Bychkov *et-al*, the one-dimensional character of the model system proposed by Little makes it a unique problem in which there exists a built-in coupling between superconducting and dielectric instabilities. It follows that each of these instabilities cannot be considered separately in the mechanism proposed by Little in one dimension and last but not least, fluctuations should be very efficient in a 1D conductor to suppress any long range ordering to very low temperature. These

remarks proved to be very pertinent for the development several decades later of the adequate theoretical framework needed for organic superconductivity.

A major step was accomplished in 1970 towards the discovery of new materials for superconductivity with the synthesis by F.Wudl[27] of the new molecule tetrathiafulvalene, (TTF). This molecule containing four sulfur heteroatoms in the fulvalene skeleton can easily donate electrons when it is combined to electron accepting species. This discovery has deeply influenced the subsequent evolution of the chemistry of organic conductors.

1.3 The charge transfer period, first organic conductors

The TTF molecule containing four sulfur heteroatoms in the fulvalene skeleton can easily donate electrons when it is combined to electron accepting molecules allowing the synthesis of the first stable organic metal, the charge transfer complex, TTF – TCNQ. The system is made up of two kinds of flat molecules each forming segregated parallel conducting stacks. This compound can be recognized as an organic conductor as the orbitals involved in the conduction (π -HOMO and π -LUMO for TTF and TCNQ respectively) are associated with the molecule as a whole rather than with a particular atom with carriers in each stacks provided by an interstack charge transfer *at variance* with other organic conductors such as the doped conjugated polymers.

The announcement of a large and metal-like conduction in TTF – TCNQ was made in 1973, simultaneously by the Baltimore[28] and Pennsylvania[29] groups. The Pennsylvania group made a provocative claim announcing a giant conductivity peak of the order of $10^5 (\Omega cm)^{-1}$ at 60 K arising just above a very sharp transition towards an insulating ground state at low temperature. This conductivity peak was attributed by their authors to precursor signs of an incipient superconductor. Unfortunately, the conductivity peak with such a giant amplitude could never be reproduced by other groups who anyway all agreed on the metallic character of this novel molecular material[30]. Besides, the Orsay group showed from X-ray scattering studies that the metal insulator transition at 59 K was the consequence of the instability of a conducting chain predicted by Peierls[31]. The X-ray diffuse scattering study did provide an important information namely, the band filling of TTF – TCNQ is incommensurate with a charge transfer of $\rho = 0.59$ at 300 K[31].

It is the study of transport properties under pressure which settled the origin of the conductivity peak of the conducting phase before the Peierls transition at 59. Driving the charge transfer through a commensurate value $\rho = 2/3$ under the pressure of ≈ 18 kbar provided the proof for collective Fröhlich fluctuations in a 1D regime leading in turn to a large enhancement of the ordinary single particle conduction as long as the wave length of these CDW fluctuations is not commensurate with the underlying lattice *in particular* under ambient pressure[32], see fig(2). High pressure appeared to be a parameter far more influential for organic conductors than for regular metals, it suppressed the onset of the Peierls instability in TTF – TCNQ [34] but

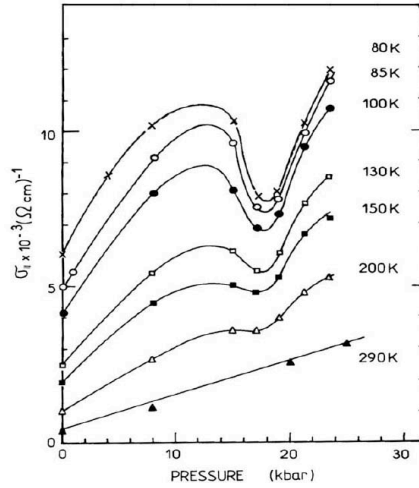


Fig. 2 Isothermal pressure dependence of the longitudinal conduction of TTF – TCNQ showing a drop of the conduction in the commensurability (x3) domain of the fluctuating Fröhlich contribution due to pinning by the lattice[33]. The ratio $\sigma(80K)/\sigma(290K)$ is evolving from 18 to 3 from ambient pressure up to 18 kbar and rising again at higher pressures.

failed to reveal any sign of superconductivity possibly with a high T_c as expected from the work of Horovitz *et-al*[35] when phonons become soft in the vicinity of the Peierls transition.

The Orsay high pressure experiments on TTF – TCNQ have been extended recently up to the pressure domain of 80 kbar by the Osaka group[34] as shown on fig(3). The early high pressure Orsay results up to 30 kbar with commensurability arising around 18 kbar have been confirmed but in addition the Peierls transition is suppressed down to 31 K at 80 kbar, probably an effect of increased interstacks coupling.

Furthermore, the role of 1D electron-electron repulsive interactions has been recognized by the $4k_F$ signature in X-ray diffuse scattering experiments[36]. Since decreasing the size of the Coulombic repulsion is expected to boost the conductivity of metals, other synthetic routes have then been followed. In the 1970s, the leading ideas governing the search for new materials likely to exhibit good metallicity and possibly superconductivity were driven by the possibility to minimize the role of electron-electron repulsions and at the same time to increase the electron-phonon interaction while keeping the overlap between stacks as large as possible. This led to the synthesis of new series of charge transfer compounds which went beyond the known TTF – TCNQ system, for example changing the molecular properties while retaining the same crystal structure. It was recognized that the electron polarizability is important to reduce the screened on-site electron-electron repulsion and that the redox potential $(\Delta E)_{1/2}$ should be minimized, [37,38] in order to fulfill this goal. Hence, new charge transfer compounds with the acceptor TCNQ were synthesized using other heteroatoms for the donor molecule, *i.e.* substituting sulfur

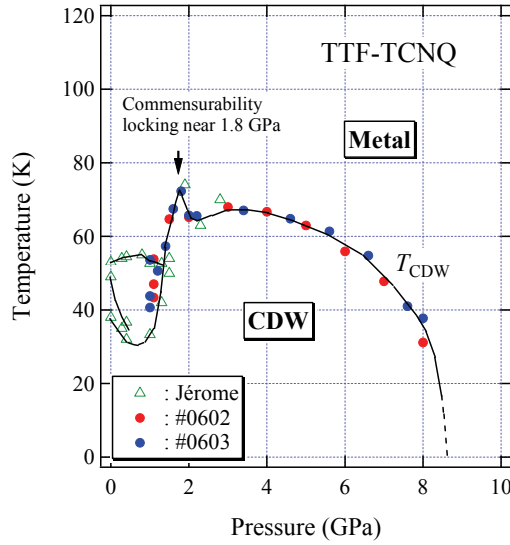


Fig. 3 Phase diagram of TTF – TCNQ under pressure measured by the Osaka group[34] including the early Orsay data[32] up to 30 kbar. The position of the peak at ≈ 18 kbar for the Peierls transition corresponds to the dip of longitudinal conduction on fig(2).

for selenium in the TTF skeleton thus leading to the TSF molecule where S stands for selenium Se.

Much attention was put on the tetramethylated derivative of the TSF molecule which, when combined to the dimethylated TCNQ gave rise to TMTSF-DMTCNQ[39]. The outcome of the high pressure study of this latter compound has been truly decisive for the quest of organic superconductivity [39,40,41]. First, the metal insulator transition located at 42 K has been identified by X-ray diffuse scattering experiments[42] as a Peierls transition driven by the TMTSF chain and a quarter filling of both donor and acceptor bands of this charge transfer compound has been derived from the measurement of the wave vector $2k_F$ in the Peierls state. Second, for the first time the metallic state of an organic compound could be stabilized down to 1.2 K under pressure *albeit* without superconductivity [43]. Even if the reason for the stability of a metallic state in TMTSF-TCNQ above the pressure of 9 kbar is not fully established at the moment emphasizing the role of the donor stack (TMTSF) has been a strong motivation for the synthesis of new organic conductors with structures even simpler than those of two stacks charge transfer compounds. Fortunately, the Montpellier group[44] had synthesized in 1978 a series of isomorphous radical cationic conductors based on TMTTF (the sulfur analog of the TMTSF molecule) with an inorganic anion namely, $(TMTTF)_2X$. These materials were all insulating at ambient pressure although some of them did reveal superconductivity under pressure much later and became quite important for studying the physics of 1D conductors since it is the replacement of

TMTTF by TMTSF in the stoichiometric $(\text{TM})_2\text{X}$ salt which opened the door to organic superconductivity[45].

2 A breakthrough in the eighties

At the same time, the Copenhagen group led by Klaus Bechgaard and experienced with the chemistry of selenium succeeded in the synthesis of a new series of conducting salts all based on the TMTSF molecule namely, $(\text{TMTSF})_2\text{X}$ where X is an inorganic mono-anion with various possible symmetry, spherical (PF_6 , AsF_6 , SbF_6 , TaF_6), tetrahedral (BF_4 , ClO_4 , ReO_4) or triangular (NO_3)[45]. All these compounds but the one with $\text{X} = \text{ClO}_4$ did reveal an insulating ground state under ambient pressure. What is so special with $(\text{TMTSF})_2\text{PF}_6$

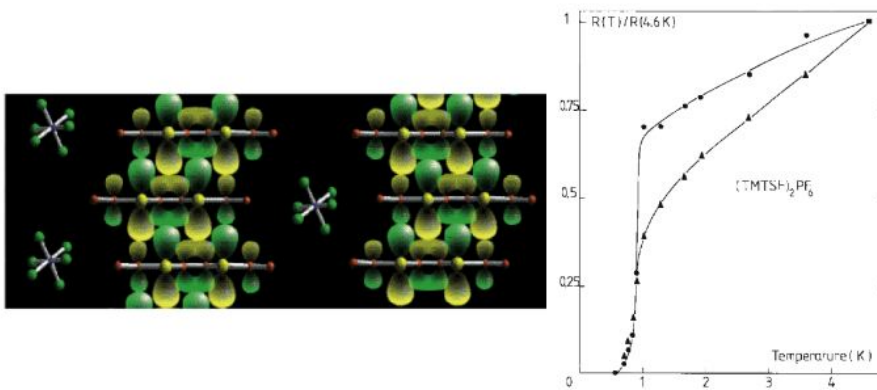


Fig. 4 Side view of $(\text{TMTSF})_2\text{ClO}_4$ along the b axis. The structure of $(\text{TMTSF})_2\text{PF}_6$ is similar with centrosymmetric PF_6^- anions. First observation of superconductivity in $(\text{TMTSF})_2\text{PF}_6$ under a pressure of 9 kbar[46]. The resistance of two samples is normalized to the 4.5 K value. Two features are abnormal for the resistance of ordinary metals at low temperature, the strong temperature dependence below 4 K and the sublinear behaviour above T_c . They are both extensively discussed in Secs (3.4.1 and 3.4.3).

, the prototype of the so-called Bechgaard salts, unlike previously investigated TTF – TCNQ, is the magnetic origin of the ambient pressure insulating state[47] contrasting with the Peierls-like ground states discovered until then. The ground state of $(\text{TMTSF})_2\text{PF}_6$ turned out to be a spin density wave state similar to the predictions of Lomer[48] and Overhauser[49] for metals. The onset of itinerant antiferromagnetism opens a gap at Fermi level and since the Fermi surface is nearly planar the gap develops over the entire surface. The magnetic origin of the insulating ground state of $(\text{TMTSF})_2\text{PF}_6$ was thus the first experimental hint for the prominent role played by correlations in these organic conductors, fig(4). Superconductivity of $(\text{TMTSF})_2\text{PF}_6$ occurred at 1 K once the *SDW* insulating ground state could be suppressed under a pressure of about 9 kbar[46]. The competition between a distorted phase and super-

conductivity had already been observed for instance in the transition metal dichalcogenides layer crystals under pressure such as $2H - NbSe_2$ [50]. However, in this latter situation superconductivity preexisted in the low pressure metallic phase with a Peierls distortion due to the nesting of some regions of the Fermi surface[51] decreasing the density of states at the Fermi level. As noticed by Friedel[52] the effect of pressure on the T_c of $2H - NbSe_2$ compounds is likely to be an increase of $N(E_F)$ by reducing the gaps on some parts on the Fermi surface leading to a concomitant enhancement of T_c . It is a situation *at variance* with what is encountered in $(TMTSF)_2PF_6$ since the *SDW* phase is truly insulating. While, superconductivity is optimized at the border with the *SDW* state, the reasons are quite different from what has been suggested for layer compounds as discussed below.

2.1 A generic phase diagram

In the mid-1980's, the isostructural family comprising the sulfur molecule with the same series of monoanions was investigated under pressure and it was realized that $(TMTTF)_2X$ and $(TMTSF)_2X$ salts both belong to a unique class of materials forming the generic $(TM)_2X$ phase diagram[53], fig(5). In particular, $(TMTTF)_2PF_6$, although the most insulating compound of the phase diagram can be made superconducting at low temperatures under a pressure of 45 kbar[54,55]. The discovery of $(TMTSF)_2PF_6$ *via* the study of the generic phase diagram has thus contributed to the knowledge of 1D physics much more than the phenomenon of superconductivity in an organic conductor. Because of their particular crystal structures, such materials can be considered at first glance as prototypes for 1D physics[57], see also J. Friedel[58] for a short historical summary on the role of correlations in organic conductors.

What 1D physics means in a nutshell, is the replacement of Landau-Fermi quasiparticles low lying excitations by decoupled spin and charge collective modes [59,60]. The model for 1D conductors starting from a linearized energy spectrum for excitations close to the Fermi level and adding the relevant Coulomb repulsions which are responsible for electron scattering with momentum transfer 0 and $2k_F$ is known as the popular Tomonaga-Luttinger (TL) model. In this model the spatial variation of all correlation functions (spin susceptibility at $2k_F$ or $4k_F$, *CDW*, Superconductivity) exhibit a power law decay at large distance, characterized by a non-universal exponent K_ρ (which is a function of the microscopic coupling constants)[61]. However an important peculiarity of $(TM)_2X$ materials makes them different from the usual picture of TL conductors. Unlike two-stacks TTF – TCNQ materials, $(TM)_2X$ conductors exhibit a band filling which is commensurate with the underlying 1D lattice due to the 2:1 stoichiometry imposing half a carrier (hole) per TM molecule. Consequently, given a uniform spacing of the molecules along the stacking axis the unit cell contains 1/2 carrier, *i.e.* the conduction band is quarter-filled. However, non-uniformity of the intermolecular spacing had

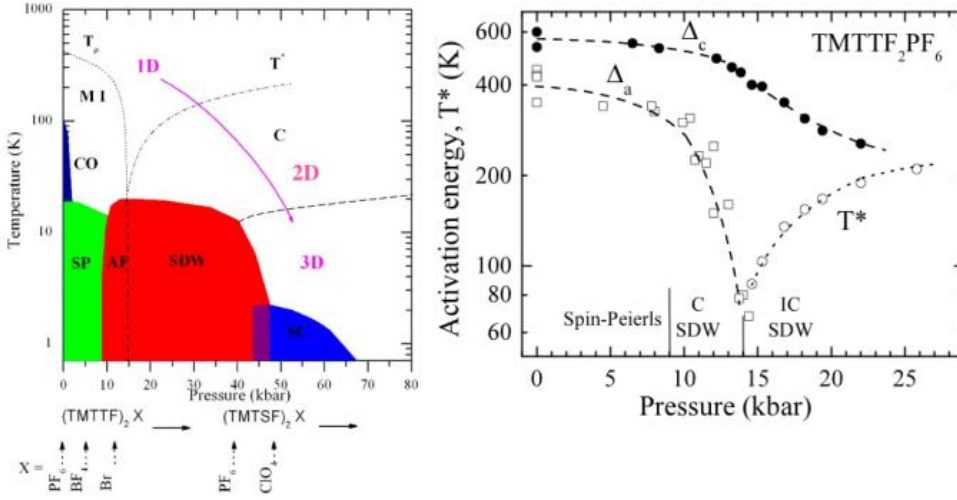


Fig. 5 Left. Generic phase diagram for $(\text{TM})_2\text{X}$ compounds[53] based on the sulfur compound $(\text{TMTTF})_2\text{PF}_6$ under ambient pressure as origin for the pressure scale. Phases with long range order are shaded. T_p and T^* mark the onset of 1D charge localization and 1D/2D deconfinement respectively. The dashed line between 2D and 3D regimes defines the low temperature domain for 3D coherence. Right. Pressure dependence of the transport activation. The activation for the c axis transport (Δ_c) although decreasing under pressure survives up to high pressures while the longitudinal transport (Δ_a) is no longer activated above 15 kbar when a dimensional cross-over occurs at the temperature T^* [56].

been noticed from the early structural studies of $(\text{TMTTF})_2\text{X}$ crystals[62] due to the periodicity of the anion packing twice the periodicity of the molecular packing. This non-uniformity provides a dimerization of the intrastack overlap which is important in the sulfur series (prominent $1/2$ Umklapp scattering) but still present although less developed in some members of the $(\text{TMTSF})_2\text{X}$ series.

An important consequence of the commensurate situation for $(\text{TM})_2\text{X}$ materials is the existence of localization channels due to electron-electron Umklapp scatterings with momentum transfer $4k_F$ (two particles scattering) or $8k_F$ (four particles scattering) corresponding to half or quarter-filled bands respectively[63,64]. This localization is a typical outcome of 1D physics in the presence of repulsive interactions and leads to a charge gap Δ_ρ in the quasiparticle spectrum although no ordering is expected at any finite temperature for a purely 1D system. The spin sector remains gap-less on account of the separation between spin and charge degrees of freedom in 1D conductors. Fortunately, most features of the 1D localization and the physical properties of this electron gas can be studied by transport and optical properties of the materials. The most salient effect is the existence of a minimum of resistance at T_p below which the resistance becomes activated. According to the theory of the commensurate 1D electron gas worked out by a number of authors, using the extended Hubbard, DMRG and bosonisation models, (see references[65,66] for

further reading) it has been shown that both Umklapp mechanisms compete for the establishment of the charge gap, $1/4$ and $1/2$ Umklapp scatterings leading to charge ordered and Mott insulators respectively[67].

As long as the carriers are localized on individual stacks, the Mott gap prevents the formation of electron hole pairs and in turn any hopping to neighboring stacks[68,65]. Therefore, even if a finite interchain coupling t_b already exists according to the band structure calculation in real materials, it is not recognized as a pertinent quantity. The carriers are confined on individual stacks as long as Δ_ρ remains finite. The 1D confinement is affected by pressure due first to the weakening of the correlations and second by the interplay between the 1D localization and the single particle interchain hopping t_b . Once the interchain single particle hopping (increased by pressure) reaches the order of magnitude of the Mott gap, confinement ceases and the existence of a quasi-1D Fermi surface becomes meaningful[64,69,70]. In some respects the deconfinement observed under pressure around 15 kbar on fig(5) is the signature for a crossover from strong to weak coupling in the generic phase diagram. The Néel phase turns into an ordered weak antiferromagnet (spin density wave) at the deconfinement pressure.

On the left side of the generic diagram the Mott localization, the consequence of Umklapp scattering as a one dimensional effect in a TL electron gas does not establish long order. Various types of range orders occur only at low temperature in this 1D Mott-localized sector.

On the very left side of the generic diagram on fig(5) a phase transition towards a long range ordered insulating phase has been observed in the charge-localized temperature sector. This phase at low temperature has been ascribed, according to NMR data, to the onset of a charge disproportionation between molecules on the molecular chains[71]. Since the charge of this low temperature phase (*see*, the CO state on the left side of the generic (TMTTF)₂PF₆ diagram, figure (5)), is no longer uniform ferroelectricity can be expected as shown by a signature in dielectric measurements[72]. The stability of the CO state (often called a Wigner state) is a direct consequence of the long range nature of the Coulomb repulsion which, in terms of the extended Hubbard model, amounts to finite on-site U and second-neighbours V repulsions. Increasing pressure, spins localized on dimers of molecules couple to the lattice and formed a spin-Peierls ground state evolving possibly through a quantum critical point[73] into a Néel antiferromagnetic phase under pressure.

2.1.1 The generic diagram studied by transport

Regarding the upper part of the diagram on fig(5) a metal-like behaviour of the longitudinal resistance is still be observed at T larger than Δ_ρ leading to a resistance displaying a power law $\rho(T) \approx T^\theta$ ($\theta > 0$). Experimental studies have revealed such a metallic behaviour for the resistance either in (TMTTF)₂X under pressure[56, 74] or in (TMTSF)₂X even at ambient pressure[33]. What has been found is a sublinear exponent, namely $\alpha = 0.93$ for the constant volume temperature dependence of the (TMTSF)₂PF₆ resistance[56, 74].

Transport experiments can be explained within the theoretical framework of commensurate conductors with commensurability one or two. However, in the case of half-filling (commensurability one) the Luttinger parameter K_ρ should be very close to unity (very weak repulsive interactions) since $\theta = 4K_\rho - 3$. A situation which implies weak coupling $K_\rho \approx 1$ (nearly free electrons) would be hard to reconcile with the exchange enhancement of the spin susceptibility, an other sign for the role of correlations[69]. On the other hand, when quarter-filled Umklapp scatterings prevail at high temperature $\theta = 16K_\rho - 3$ and consequently $K_\rho = 0.23$ according to the data of $(\text{TMTSF})_2\text{PF}_6$.

Other arguments in favour of a predominance of the quarter-filled Umklapp scattering above T_ρ are given by two additional experimental features.

First, the phase diagram of an organic salt $(\text{EDT} - \text{TTF} - \text{CONMe}_2)_2\text{AsF}_6$ in which for symmetry considerations (the absence of inversion center between adjacent molecules along a stack and the existence of a glide plane symmetry[75]) dimerization is prevented, hence 1/4- Umklapp scattering is the only channel left to explain the carrier localization in this 1D conductor. In spite of the different structures the high temperature limit of phase diagrams of $(\text{EDT} - \text{TTF} - \text{CONMe}_2)_2\text{AsF}_6$ and $(\text{TM})_2\text{X}$ are fairly similar[76].

Second, the temperature dependence of the transverse conduction along the least conducting c direction which displays an insulating behaviour below room temperature going through a maximum around $T^* \approx 80 - 100$ K and becoming metallic at lower temperatures. In this metallic regime the transverse resistance is remaining several orders of magnitude above the Mott-Ioffe critical value which is considered as the limit between metal and insulating-like transport [77].

As long as coherence is not established between 2 D planes, transverse transport requires tunneling of Fermions (*at variance* with the longitudinal transport which is related to 1D collective modes) between neighbouring chains and therefore probes the amount of quasi particles (QP) existing close to Fermi level. The insulating character of the transverse transport at high temperature can thus be interpreted as the signature of a non Fermi-Landau behavior [78]. When transport along the c -direction is incoherent, **transverse conductivity probes the physics of the $a - b$ planes** namely, the physics of the weakly interacting Luttinger chains in the $a - b$ planes. The resistivity along the least conducting direction depends on the one-electron spectral function of a single chain and reads $\rho_c(T) \approx T^{1-2\alpha}$ [79] where α is related to K_ρ , ($\alpha = \frac{1}{4}(K_\rho + 1/K_\rho - 2)$). It is again a K_ρ of about 0.25-0.30 which is found experimentally in $(\text{TMTSF})_2\text{PF}_6$ [78].

2.1.2 1D-2D crossover

The temperature T^* where the c^* -axis transport switches from an insulating to a metallic temperature dependence corresponds to a cross-over between two regimes, see fig(5); a high temperature regime with no QP weight at Fermi energy (possibly a TL liquid in the 1D case) and another regime in which

the QP weight increases with decreasing temperature. This picture does not necessarily imply that the transport along the c -direction must also become coherent below the cross-over since the c -axis transport may remain incoherent with a progressive establishment of a Fermi liquid in $a - b$ planes at temperatures below T^* . Consequently, the temperature dependence of transport properties along a and c -axes in the 1D regime above T^* lead to a determination of K_ρ of order 0.23 in $(\text{TMTSF})_2\text{PF}_6$ and $(\text{TMTTF})_2\text{PF}_6$ under a pressure of 12-15 kbar respectively. The Luttinger parameter is much smaller in $(\text{TMTTF})_2\text{PF}_6$ at ambient pressure[56], ($K_\rho=0.18$) due to the enhancement of correlations in the left region of the phase diagram, fig(5). Optical data measured throughout the entire generic diagram reach fairly similar conclusions[80].

The decrease of the charge gap under pressure, fig (5), is due to a weakening of intra chain correlations moving from left to right in the diagram. Carriers are confined on the 1D chains and the transverse coupling renormalized by intrachain interactions is not pertinent[81].

However, when this gap becomes of the order of the bare kinetic transverse coupling a close interplay between this gap and the transverse coupling occurs giving rise to the sharp suppression of the localization observed around 15 kbar in $(\text{TMTTF})_2\text{PF}_6$. At higher pressures the transverse coupling becomes pertinent and approaches the bare coupling which is increasing only smoothly under pressure. The deconfinement of the carriers is observed around T^* . Below this deconfinement temperature charge excitations lose their 1D character and resemble more and more what is expected in Fermi liquids (quasiparticles), leading in turn to a quadratic temperature dependence for the longitudinal resistivity. However, electron excitations of this "Fermi liquid" retain a low energy gap in the far infra-red spectrum in which most of the oscillator strength is carried by states above the gap coexisting with a very narrow and intense zero frequency peak in the conductivity[82,83].

2.1.3 2D-3D crossover

A three dimensional anisotropic coherent picture seems to prevail at low temperature in $(\text{TMTSF})_2\text{X}$ compounds according to the Kohler's rule [84] and angular magnetoresistance oscillations observed in $(\text{TMTSF})_2\text{ClO}_4$ and $(\text{TMTSF})_2\text{PF}_6$ under pressure[85,86,87,88]. In addition, optical reflectance data of light polarised along c^* support the existence for $(\text{TMTSF})_2\text{ClO}_4$ of a weak Drude behaviour in the liquid helium temperature domain when $k_B T < t_{\perp c}$ [89]. However, the upper limit for the temperature domain of 3D coherence has been established comparing the temperature dependence of the resistivity along a and c^* . This 3D to 2D crossover domain is defined by the temperature above which temperature dependences of both components of transport cease to be identical[90]. The 3D coherence regime is plotted on the generic diagram of figure(5).

2.1.4 The generic diagram studied by optics

It is remarkable that most features of the generic phase diagram presented on fig(5) are very well recovered by the study of low frequency excitations via the far infra red optical conductivity investigations performed on either different materials of the $(\text{TM})_2\text{X}$ series or on a given compound under pressure. Compounds on the left of the diagram exhibit a charge gap E_{gap} due to the 1D Mott localization, $E_{\text{gap}}=1100$ and 375 K for $(\text{TMTTF})_2\text{PF}_6$ and $(\text{TMTTF})_2\text{Br}$ respectively[74]. These values for the optical gap are indeed in fairly good agreement with the DC transport activation energy shown on fig(5) since $2\Delta_{\text{activation}} = E_{\text{gap}}$. Moving towards right in the phase diagram, the optical evolves and resembles at low temperature the spectrum expected in doped Mott semiconductor, see fig(6), namely, a high frequency component at $\omega > t_b$ carrying most of the oscillator strength, a correlation pseudogap located around 275 K and a narrow Drude peak carrying about 1% of the total oscillator strength[91]. The high temperature 1D TL properties of the system are

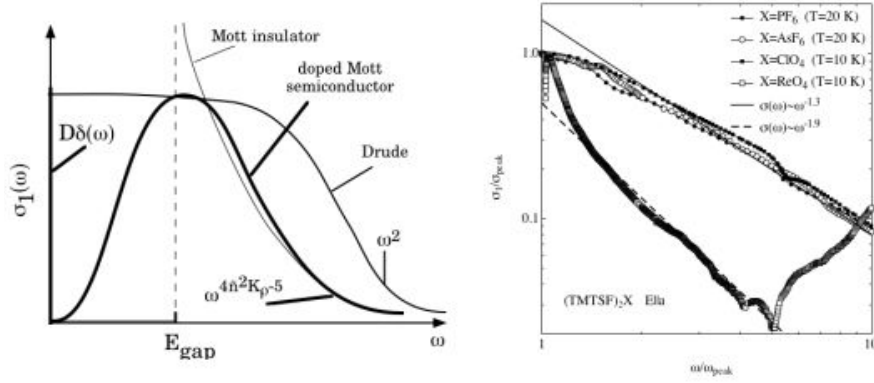


Fig. 6 (Left) Optical conductivity of a Mott insulator and of a doped Mott semiconductor[66]. The power law decay of the optical conductivity at high frequency depends on the Luttinger parameter K_ρ . (Right) Power law behaviour of the optical conductivity for various $(\text{TM})_2\text{X}$ compounds measured in the metallic phase at low temperature (except for ReO_4^- which is an insulator due to the anion ordering below 180 K), according to references[91,92].

consistently observed through the power law frequency dependence of the conductivity at high frequency above the correlation pseudogap, $\sigma(\omega) \approx \omega^{-\gamma}$ with $\gamma = 1.3$ [83]. Such an exponent is actually in good agreement with transport data of the selenide series since $K_\rho = 0.23$ is recovered given the known relation $\gamma=5-16K_\rho$ when quarter-filled band Umklapp scattering is dominant[64].

The investigation of the pressure and temperature dependence of the optical conductivity of $(\text{TMTTF})_2\text{PF}_6$ and $(\text{TMTSF})_2\text{PF}_6$ [80,93] has also identified for $(\text{TMTTF})_2\text{PF}_6$ a Mott deconfinement when the Mott gap is approx-

imately twice t_b and a dimensional crossover at T^* for both systems revealed by the development of a Drude type response along b .

Although not much work has been devoted to the optical response along the c^* direction the study performed on $(\text{TMTSF})_2\text{ClO}_4$ by Henderson *et al*[89] indicates that this compound is a 2D metal above 10K and that a small Drude response emerges at lower temperature characteristic of a 3D anisotropic electron gas.

3 The last five years

At the turn of the 21st century, the prominent role of AF fluctuations in the metallic phase next to the *SDW* phase and the proximity between superconductivity and the magnetically ordered phase were both well established experimentally[94,95]. In addition, one was wondering about a possible connection between magnetism and electron pairing but even the symmetry of the *SC* order parameter was a very controversial topic.

On the one hand early NMR studies had concluded to nodal superconductivity in $(\text{TMTSF})_2\text{ClO}_4$ [96] *at variance* the with more recent Knight shift measurements in $(\text{TMTSF})_2\text{PF}_6$ suggesting triplet *p*-type pairing[97]. This latter possibility was actually in line with the claim of superconductivity surviving for certain orientations of the magnetic field beyond the field set by the Pauli limiting field $\mu_0 H_P \sim 2.5$ T where ordinary singlet pairs would become unstable on account of the Zeeman splitting for a T_c of 1.2 K. On the other hand a thermal conductivity study of $(\text{TMTSF})_2\text{ClO}_4$ concluded to a nodeless superconductivity[98] not necessarily associated to *s*-wave superconductivity as odd parity such as a *p*-wave gap could explain the behaviour of temperature dependence of thermal conductivity.

The clue could not come from a single experiment but from a coordinated experimental program with NMR in the superconducting state at UCLA[99], a study of the role of non magnetic impurities on T_c at Orsay[100], field angle resolved calorimetry at Kyoto[101] and the study of transport in the metallic phase surrounding superconductivity at Sherbrooke[102,103]. These questions will be addressed in the rest of this paper.

3.1 NMR in the superconducting phase

Regarding the spin part of the *SC* wave function, a triplet pairing was first claimed from a divergence of the critical field H_{c2} exceeding the Pauli limiting value reported at low temperature in $(\text{TMTSF})_2\text{PF}_6$ under pressure when H is applied along the b' or a axes [104] and from the absence of any change in the ^{77}Se Knight shift at T_c [105].

However more recent experiments performed at fields lower than those used in reference[105] for the work on $(\text{TMTSF})_2\text{PF}_6$ did reveal a clear drop of the ^{77}Se Knight shift below T_c in the compound $(\text{TMTSF})_2\text{ClO}_4$ [99]. These

new data provided a conclusive evidence in favour of singlet pairing, (Fig.7). In addition, a step increase of the spin lattice relaxation rate versus magnetic field for both field orientations $\parallel a$ and b' provided evidence for a sharp cross-over or even a phase transition occurring at low temperature under magnetic field between the low field d -wave singlet phase and a high field regime exceeding the paramagnetic limit H_p being either a triplet-paired state[106,107] or an inhomogenous Fulde-Ferrell-Larkin-Ovchinnikov state[108,109].

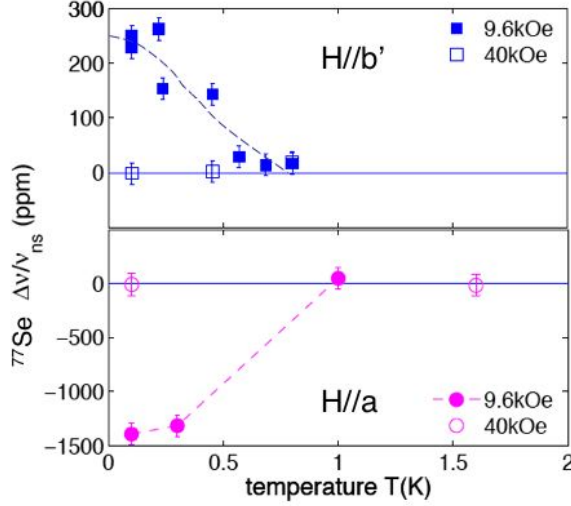


Fig. 7 ^{77}Se Knight shift vs T for $(\text{TMTSF})_2\text{ClO}_4$, for $H//b'$ and a , according to reference [99]. The sign of the variation of Knight shift at T_c depends on the sign of the hyperfine field. A variation is observed only under low magnetic field. The difference of T_c for the two field orientations is due to the anisotropy of H_{c2} . The field of 4T is still lower than the critical field derived from the onset of the resistive transition ($H_{c2} \approx 5T$), *vide* Sec().

3.2 Organic superconductivity and non magnetic impurities

The recent finding of a T_c strongly affected by the value of the elastic electron lifetime in the presence of non magnetic lattice defects has conclusively ruled out the s -wave hypothesis and suggested the existence of nodes with zeros of the SC gap on the Fermi surface[100].

Leaving the cation stack uniform in order to preserve the electronic structure, a soft way of introducing non magnetic disorder scattering centers can be achieved by playing on the anion stacks. The role of the anion stack on the ground state is enhanced as soon as the anion located at an inversion center of the structure does not possess a central symmetry[110]. This is the case in particular for tetrahedral anions such as $X = \text{ClO}_4$ which order at low temperature ($T_{AO}=24\text{K}$) in line with entropy minimization. As anion reorientation

requires a tunneling process between two states at equal energy but separated by a large potential barrier, the dynamics of orientation is a slow process at low temperature and becomes even slower under pressure when the tunneling barrier increases. Hence, for samples slowly cooled through T_{AO} (in the so-called R-state) the orientation of the anions is uniform along the stacking axis but alternate along the b-direction leading in-turn to a doubled periodicity with a concomitant opening of an energy gap Δ_{anion} on the Fermi surface at $\pm\pi/2b$ and the creation of two sheets of open Fermi surfaces at $+k_F$ and $-k_F$ respectively. Fast cooled samples on the other hand reach low temperature in a state (the Q-state) where orientational disorder is frozen-in. The superconducting state arises at a depressed T_c in a sample where homogenous anion-oriented domains coexist with anion disorder outside of these domains[111]. When the cooling rate becomes fast enough in a Q state full disorder of the anions is preserved ($\xi_{anion} < v_F/\Delta_{anion}$) and the single-sheet warped Fermi surface of the high temperature structure prevails at low temperature leading in turn to the instability of the metallic phase against a *SDW* ground state at $T_{SDW}=5K$ [111]. Furthermore, it has been shown that neither the Pauli susceptibility[112] nor the density of states[113] of the normal phase are affected by the orientational disorder introduced by the fast cooling procedure as long as a superconducting ground state is observed.

An other approach for the introduction of anionic disorder has been successful with the synthesis of an anionic solid solution involving anions of similar symmetry.

The early studies by Tomić *et-al* [111] in $(TMTSF)_2(ClO_4)_{(1-x)}(ReO_4)_x$ have shown that both the low temperature conductivity and the transition towards superconductivity are very strongly affected by alloying although X-ray investigations have revealed that long range order is preserved up to 3% ReO_4^- with a correlation length $\xi_a > 200\text{\AA}$ [114]. Single crystals of this solid solution with x in the range $0 \leq x \leq 0.17$ have been prepared with the usual electrocrystallization technique and studied for their behaviour at low temperature in a dilution fridge. Up to about 6% ReO_4^- nominal concentration a *SC* transition is observed although depleted from the T_c in pristine samples. Meanwhile, an insulating ground state is stabilized above 10% ReO_4^- or so. The critical temperature has been determined from the temperature where H_{c2} reaches a zero value, see figure (8).

The data of fig (8) show that the slope dH_{c2}/dT follows T_c as this latter quantity is decreased upon alloying. This is the behaviour expected in a clean type II superconductor[115], but in such a situation T_c itself should not be affected by non magnetic impurities.

At higher impurity content, ($x=15\%$) a new behaviour has been observed. The anions still order below T_{AO} remaining of the order of 24K as indicated by the concomitant drop of the residual resistivity (although smaller than what is observed in pristine samples). An upturn of the resistivity noticed at low temperature in the R-state can be ascribed to the onset of an insulating ground state at 2.35 K (as defined by the maximum of the logarithmic derivative of

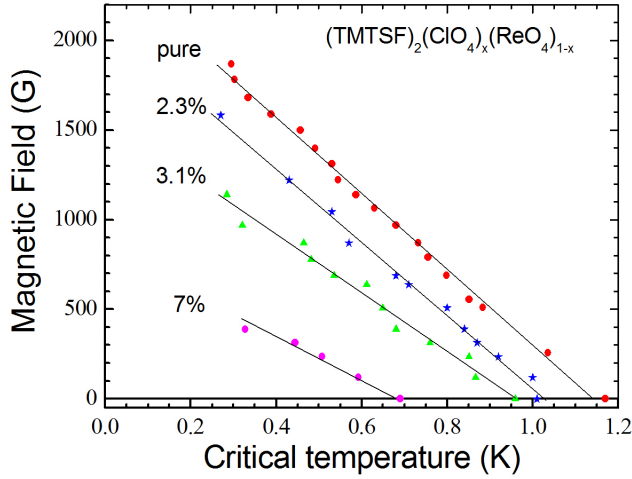


Fig. 8 Critical field H_{c2} for $(\text{TMTSF})_2(\text{ClO}_4)_{1-x}(\text{ReO}_4)_x$ alloys with different concentrations of ReO_4^- all slowly cooled in the R state.

the resistance *versus* T). A summary of this investigation is displayed on fig (9) where T_c is plotted against the residual (elastic) resistivity ρ_0 .

However, the determination of the elastic contribution is by no means an easy task. As the field of organic superconductors were developing over the years several situations regarding the behaviour of the resistivity of the metallic phase close to T_c could be obtained ranging from the classical T^2 Fermi liquid behaviour to a linear temperature dependence and even to a sublinear temperature dependence in the vicinity of T_c . The residual resistivity on fig (9) has been determined by the extrapolated value to zero temperature of the linear behaviour observed below 4K. The suppression of T_c is clearly related to the enhancement of the scattering rate in the solid solution. Since the additional scattering cannot be ascribed to magnetic scattering according to the EPR checks showing no additional traces of localized spins in the solid solution, the data in figure (9) cannot be reconciled with the picture of a superconducting gap keeping a constant sign over the whole $(\pm k_F)$ Fermi surface. They require a picture of pair breaking in a superconductor with an unconventional gap symmetry. The conventional pair breaking theory for magnetic impurities in usual superconductors has been generalized to the case of non-magnetic impurities in unconventional materials and the correction to T_c obeys the following relation [116,109],

$$\ln\left(\frac{T_c^0}{T_c}\right) = \psi\left(\frac{1}{2} + \frac{\alpha T_c^0}{2\pi T_c}\right) - \psi\left(\frac{1}{2}\right), \quad (1)$$

with $\psi(x)$ being the Digamma function, $\alpha = \hbar/2\tau k_B T_c^0$ the depairing parameter, τ the elastic scattering time and T_c^0 the limit of T_c in the absence of any scattering. The experimental data follow the latter law with a good accuracy

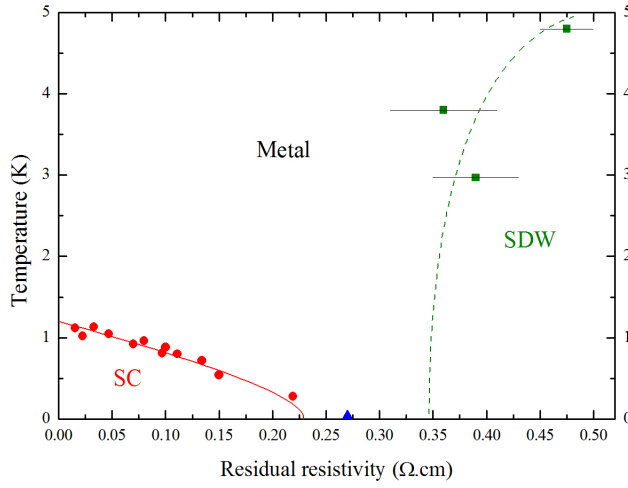


Fig. 9 Phase diagram of $(\text{TMTSF})_2(\text{ClO}_4)_{(1-x)}(\text{ReO}_4)_x$ governed by non magnetic disorder according to reference[100]. All circles refer to very slowly cooled samples in the R-state with different ReO_4^- contents. The triangle at $T = 0\text{K}$ for the sample of $\rho_0 = 0.27(\Omega\text{cm})^{-1}$ is metallic down to the lowest temperature of the experiment. When an upturn of the resistivity is observed signaling the onset of a *SDW* state no sign of superconductivity can be noticed down to the lowest temperature. The continuous line (red) is a fit of the data with the Digamma function and $T_c^0 = 1.23\text{K}$.

with $T_c^0 = 1.23\text{K}$. The influence of non magnetic impurities on the superconducting phase implies the existence of positive as well as negative values for the *SC* order parameter. It precludes the usual case of *s*-symmetry but is unable to discriminate between two possible options namely, singlet-*d* (*g*) or triplet-*p* (*f*)[117], see fig(10).

Symmetry	s	p	d	f	g
Sensitivity to impurities		✓	✓	✓	✓
NMR Knight shift and $1/T_1$	✓		✓		✓
Doppler shift			✓	(✓)	✓

Fig. 10 Possible gap symmetries agreeing with the different experimental results. The *d*-wave (or *g*-wave) symmetry is the only symmetry agreeing with all experiments, (yellow column on line).

3.3 Doppler shift and paramagnetic limitation

The response of superconductivity to non magnetic impurities and the loss of spin susceptibility at T_c should be sufficient to qualify the d -wave alternative as the likely one among the various possibilities displayed on fig (10). In such a case, nodes of the gap should exist on the Fermi surface and could be located.

This has been made possible via a measurement of the quasi particle density of states in the superconducting phase performed in an oriented magnetic field[101]. This experiment is based on a Volovik's important remark[118] that for superconductors with line nodes, most of the density of states in their mixed state under magnetic field comes from the superfluid density far outside the vortex cores. The energy of QP's in the superfluid density rotating around the vortex core with the velocity $\mathbf{v}_s(\perp H)$ is Doppler-shifted by the magnetic field and reads,

$$\delta\omega \propto \mathbf{v}_s \cdot \mathbf{v}_F(\mathbf{k}) \quad (2)$$

where $\mathbf{v}_F(\mathbf{k})$ is the Fermi velocity at the \mathbf{k} point on the Fermi surface. The Doppler shift can contribute to the DOS in the superconducting state as long as it remains smaller than the superconducting energy gap, *i.e* only for those \mathbf{k} states located in the vicinity of gap nodes on the Fermi surface. Hence, the contribution of the Doppler shift is minimum when the Fermi velocity at a node and the magnetic field are parallel according to eq (2), see fig(11) and should contribute to a kink in the rotation pattern of $C(\phi)$. The Doppler shift has

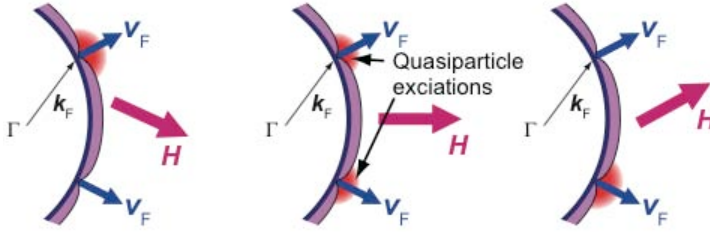


Fig. 11 Sketch of the influence of a magnetic field on the quasi particle DOS. The contribution of Doppler-shifted quasi particles to the DOS is minimum when the magnetic field is parallel to \mathbf{v}_F at one of the nodes (left or right)

already been used extensively in the case of 2D superconductors expected to reveal line nodes probing the thermal conduction or the specific heat while the magnetic field is rotated in the basal plane[119,120]. For such 2D conductors $\mathbf{v}_F(\mathbf{k})$ is usually colinear with \mathbf{k} . Therefore, the angular resolved specific heat (or thermal conductivity) enables to reveal the positions of the gap nodes according to the angles corresponding to minima of specific heat (thermal conductivity)[119].

The situation is somewhat peculiar for Q1D Fermi surface. There, anomalies in the rotation pattern of C_v are expected at angles ϕ_n between H and $\mathbf{v}_F(\mathbf{k}_n)$ where \mathbf{k}_n corresponds to a nodal position on the Fermi surface.

A simple model has been used to understand the data of angular resolved C_v of $(\text{TMTSF})_2\text{ClO}_4$ [101]. The rotation pattern has been modeled by,

$$N(\phi) \propto \sqrt{H/H_{c2}(\phi)} \Sigma_n A_n | \sin(\phi - \phi_n) | \quad (3)$$

where the first factor reproduces the anisotropic character of the critical field in the basal plane while the weighted summation over angles accounts for the existence of nodes at angles ϕ_n between the magnetic field and the special \mathbf{k}_n points where the Fermi velocity is parallel to H . The experimental observation of a rotation pattern at low field and low temperature which is non symmetrical with respect to the inversion of ϕ and the existence of kinks for $C(\phi)$ at $\phi = \pm 10^\circ$ on fig (12) have been taken as the signature of line nodes[101]. According to the band structure calculation the location of the nodes on the Fermi surface becomes $k_y \sim \pm 0.25b^*$. As the Pauli limitation is concerned, the superconducting phase diagram of $(\text{TMTSF})_2\text{ClO}_4$ established by thermodynamic experiments indicates a value for the thermodynamic H_{c2} along a of 2.5 T for $H \parallel a$ much smaller than the expected value of 7.7 T for the orbital limitation derived from the measurement of the temperature derivative of H_{c2} close to T_c for a clean type II superconductor[115]. On the other hand, along the two transverse directions orbital limitation is at work[101]. The domain of field above the paramagnetic limit up to H_{c2} derived from resistivity data where the specific heat recovers its normal state value requires further experimental investigations but it might be the signature of some *FFLO* phase as suggested by A. Lebed recently [121].

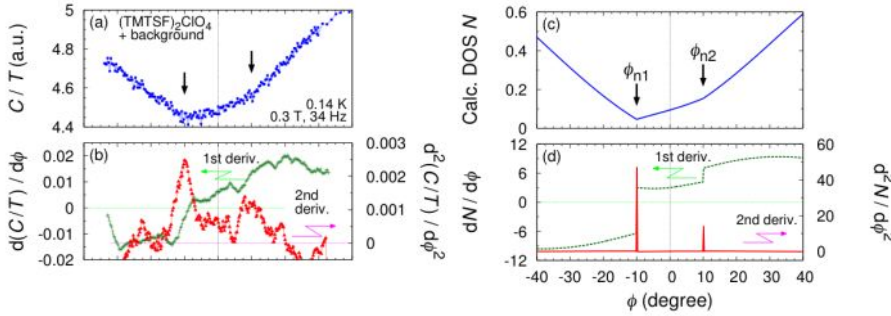


Fig. 12 Angular dependence of $C(\phi)$ and 0.3 T according to reference[101]. (a) Raw data including the background specific heat with the positions of small kinks. (b) First and second derivatives of the raw data. (c and d) Simulation of the specific heat in the vicinity of the angle $\phi = 0$ when the field is aligned along the a axis.

3.4 A Non-Fermi liquid metallic state

Let us now address a question which had been raised 30 years ago namely the non conventional behaviour of electronic transport in the metallic state in the

neighborhood of the superconducting state. It was noticed that the resistivity displays a linear temperature dependence in the low T regime becoming even sublinear in the very vicinity of the SC phase[46]. Such a behaviour is clearly not following the expectation for electron-electron scattering in a Fermi liquid where $\rho \propto T^2$ even in a 2D electron gas.

An early explanation for this non-canonical behaviour had been attributed to the existence of paraconductivity in a quasi-one dimensional conductor above T_c [122]. The calculation of Azlamazov-Larkin diagrams based on a time dependent Ginzburg-Landau theory provided, (i) a 3D domain restricted to the very vicinity of T_c where the transverse coherence extends over several interchain distances d , *i.e.*, $\xi_{\perp}/d > 1$ with $\rho_{\parallel}^{3D} \propto T^{-1/2}(\ln T/T_c)^{1/2}$ leading in turn to the classical $1/(T-T_c)^{1/2}$ divergence of the paraconductivity and, (ii) a 1D regime where $\xi_{\perp}/d < 1$ with $\rho_{\parallel}^{1D} \propto T^{1/2}(\ln T/T_o)^{-3/2}$ where T_o represents a renormalized mean field temperature, about one third of the actual mean field temperature [33].

Although the comparison between experiments and the theory for paraconducting fluctuations in reference[122] revealed a reasonable agreement in the 3D regime, it failed to reproduce the correct temperature dependence in the range 4-15K.

The reinvestigation of transport of organic superconductors was necessary after similar non Fermi liquid behaviours with T -linear laws had been reported in a lot of new superconductors discovered after 1986. This had been achieved in two steps, first clarifying transport properties experimentally and theoretically below say, 20 K and second understanding the vicinity of the superconducting transition ($\Delta T/T_c \approx 0.2$) with sublinear transport behaviour.

3.4.1 NFL, AF fluctuations, normal phase spin susceptibility, transport and superconductivity

A recent extensive study of the transport properties has been carried on in Bechgaard salts superconductors, $(\text{TMTSF})_2\text{PF}_6$ [46] and $(\text{TMTSF})_2\text{ClO}_4$ [123] as a function of pressure[102,103]. This study has focused on the electronic transport at low temperature in the low T limit. Let us first notice that the magnetic metallic background of $(\text{TMTSF})_2\text{PF}_6$ when superconductivity occurs under pressure although suppressed by the application of a magnetic field applied along the c^* axis is far from being the expectation for a Fermi liquid where a canonical Korringa law for the nuclear spin lattice relaxation namely $T_1 T = \text{constant}$ is expected. Instead, for $(\text{TMTSF})_2\text{PF}_6$ under 9 and 11 kbar the law $T_1 T = C(T + \Theta)$ is followed as shown on fig(13). The Korringa law is observed at high temperature say, above 25 K or so but the low temperature behaviour deviates strongly from the standard relaxation in paramagnetic metals.

This Curie-Weiss behaviour of the relaxation is to be observed in a 2D fluctuating antiferromagnet[124,125,126,127] with the positive Curie-Weiss temperature Θ providing the energy scale of the fluctuations. It is vanishingly

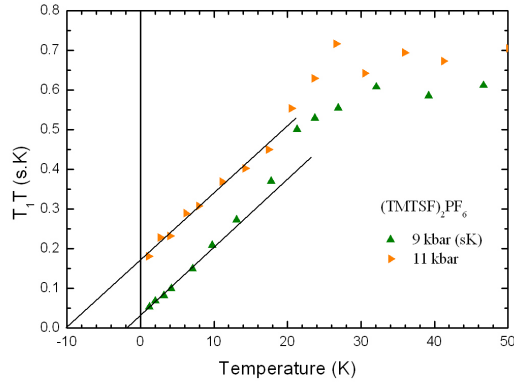


Fig. 13 Plot of the nuclear relaxation versus temperature according to the data of reference [94]. The 2D AF regime is observed below $\approx 15K$ and the small Curie-Weiss temperature of the 9 kbar run signals that this pressure is very close to a QCP probably hidden inside the *SDW/SC* coexistence domain. The Korringa regime is recovered above $30K$.

small when pressure approaches P_c but rises rapidly under pressure. The vanishing of this energy scale at P_c is thus a strong hint in favor of the existence of a magnetic quantum critical point (QCP) probably below P_c but hidden by the *SDW/SC* first order coexistence. On the other hand when Θ becomes large compared to T , the standard relaxation mechanism is recovered at low temperature in agreement with the very high pressure results. Consequently, a non standard behaviour is expected for the electron scattering at low temperature in case it is governed by spin fluctuations.

Next, when transport of the metallic phase is examined a log-log plot of the resistivity minus the residual resistivity at low temperature versus T performed at every pressure reveals at once a temperature dependence evolving from linear at low temperature to quadratic in the high temperature regime with a general tendency to become quadratic even at low temperature when pressure is well above the critical pressure P_c [102]. It is clear that in the low temperature domain where linear and quadratic behaviours of the resistivity prevail the electron scattering cannot be due to phonons since the upper limit for electron-electron scattering should fall in the range below $T < \Theta_{Debye}^2/t_{\perp}$ *e.g.*, a temperature of the order of 200 K in a conductor such as $(TMTSF)_2PF_6$.

The existence of a linear temperature dependence of the resistivity is *at variance* with the sole T^2 dependence expected from the electron-electron scattering in a conventional Fermi liquid. This is clearly seen on a log-log plot of the resistivity versus T .

An extension of the transport analysis under pressure up to higher temperatures (≈ 20 K) in $(TMTSF)_2PF_6$ [103] has suggested that the linear law is actually the low temperature limit of a polynomial behaviour. Therefore, analysing transport data with a polynom, $\rho(T) = \rho_0 + AT + BT^2$ where ρ_0

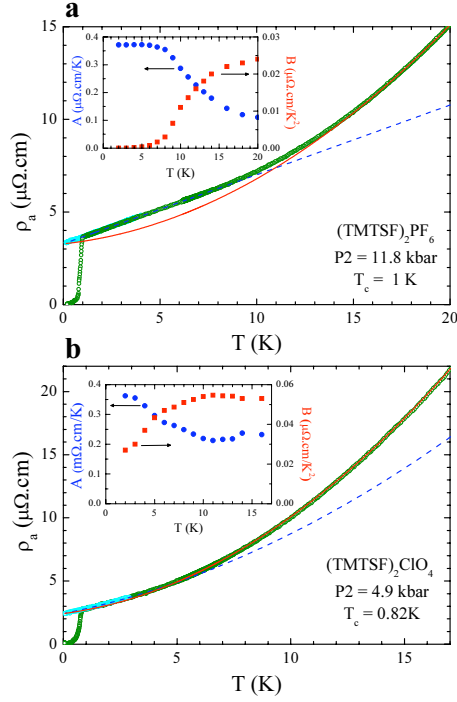


Fig. 14 Typical temperature dependence of the longitudinal resistivity of $(\text{TMTSF})_2\text{PF}_6$ below 20 K (a), and $(\text{TMTSF})_2\text{ClO}_4$ at below 17 K (b), at zero field and under $H = 0.05$ T along c^* in order to suppress SC . The second order polynomial fit, $\rho(T) = \rho_0 + A(T)T + B(T)T^2$, according to the sliding fit procedure described in reference[103] is shown for the T intervals (2 – 6) K and (18 – 22) K or (13 – 17) K in blue and red respectively. The top inserts provide the temperature dependence of the A and B coefficients.

is the linear extrapolation of the data below $4K$ under a small magnetic field suppressing SC and the prefactors A and B are determined by a sliding fit procedure[103]. Both prefactors are found to be T -dependent as displayed on fig(14).

There exists a high temperature domain ($T \geq 20$ K) in which the regular T^2 electron-electron Umklapp scattering obeys a Kadowaki-Woods law[133] and a low T regime scattering ($T \leq 8K$) where the scattering behaves more and more purely linear when pressure is close to P_c [102].

This study has first established a correlation between the amplitude of the prefactor A of the low temperature linear dependence of the resistivity and the value of the superconducting critical temperature T_c , fig(16).

Superconductivity of $(\text{TMTSF})_2\text{PF}_6$ has been observed up to the maximum pressure of this experiment (20.8 kbar) where A is still finite. A similar relation between A and T_c is obtained using the linear term of the c^* resistivity[90]. As far as $(\text{TMTSF})_2\text{ClO}_4$ is concerned, the response of T_c to high pressure is however different. A behaviour similar to that of $(\text{TMTSF})_2\text{PF}_6$ is noticed for both components of the resistivity in the low pressure domain but

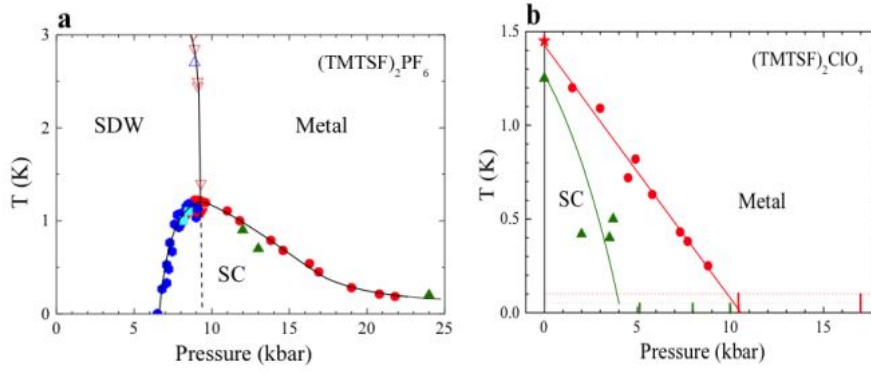


Fig. 15 (a) $(P - T)$ phase diagram of $(\text{TMTSF})_2\text{PF}_6$ deduced from resistivity measurements. The data points below 9.4 kbar (the coexistence regime) are deduced from measurements along the three crystallographic axes: down triangles for ρ_a , squares for ρ_b , hexagons for ρ_c , empty symbols for T_{SDW} and full symbols for T_{SC} [128, 129]. Above the critical pressure (9.4 kbar), only longitudinal resistivity data are plotted: (red) circles from reference [103] and (green) triangles from [130]. (b) Pressure dependence of the superconducting transition of $(\text{TMTSF})_2\text{ClO}_4$ deduced from longitudinal resistivity measurements: (red) circles from reference [103] (the star at 1 bar is derived from a ρ_c measurement [131]) and (green) triangles from [132]. Dashed-dotted horizontal lines (red or green) indicate the lowest reached temperature without superconductivity for both studies. The (red) continuous line is a linear fit of the data including the point at 1 bar. T_c for $(\text{TMTSF})_2\text{PF}_6$ although strongly decreasing under pressure does not reveal any critical pressure for the suppression of superconductivity *at variance* with $(\text{TMTSF})_2\text{ClO}_4$ in which no T_c can be detected at 10.4 and 17 kbar. Such a different behavior can be ascribed to the pair breaking effect of residual anion disorder in $(\text{TMTSF})_2\text{ClO}_4$ under pressure [100], *see text*.

the existence of a critical pressure where T_c vanishes is observed around 10.4 kbar. Such a behaviour specific to $(\text{TMTSF})_2\text{ClO}_4$ can be attributed to the remaining weak disorder of the ClO_4^- anions (even in slow cooled samples [134]) suppressing T_c when the mean distance between impurity centers and the superconducting coherence length become of the same order of magnitude as discussed in Sec(3.2). Since $(\text{TMTSF})_2\text{PF}_6$ is not concerned by this disorder effect it can be considered as an ultra pure type II superconductor.

The region of the $T - P$ phase diagram where antiferromagnetic fluctuations play a prominent role for the non elastic scattering can be conveniently defined by the temperature at which both contributions, the linear and the quadratic one are equal, $T^* = A/B$ where A and B are the values of the parameters at every pressure taken in the low and high temperature limits respectively. Figure(17) displays this strong fluctuations domain. A similar behavior is obtained for $(\text{TMTSF})_2\text{ClO}_4$ [103].

The correlation between A and T_c has suggested in turn a common origin for the inelastic scattering of the metallic phase and pairing in the SC phase $(\text{TMTSF})_2\text{PF}_6$ [135].

The decomposition of the inelastic scattering term as the sum of linear and quadratic terms rather than a power law suggests that a regular Fermi liquid

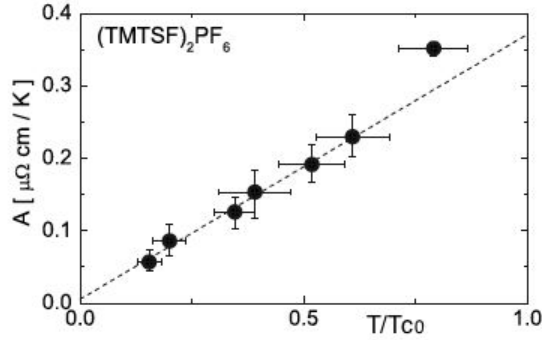


Fig. 16 Coefficient A of linear resistivity as a function of T_c plotted versus T_c/T_{c0} for $(\text{TMTSF})_2\text{PF}_6$. T_c is defined as the midpoint of the transition and the error bars come from the 10 % and 90 % points with $T_{c0} = 1.23\text{K}$ under the pressure of 8 kbar which provides the maximum T_c in the SDW/SC coexistence regime. The dashed line is a linear fit to all data points except that at $T_c = 0.87\text{K}$,

scattering channel is superimposed on a more unusual one, the latter being most likely connected to the scattering on low energy spin fluctuations.

This has been shown indeed by scaling theory for the calculation of the electron-electron scattering rate close to spin-density-wave ordering in a quasi-1D metal (the results are summarized in reference[103]). Near the critical pressure, where spin density wave connects with superconductivity (*vide infra*), spin fluctuations are strong and their spectrum is sharply peaked at very low energy ω_{sf} , which is comparable to or smaller than temperature T (see, *e.g.*, reference[127]). Under these conditions, their contribution yields a clear linear temperature dependence for the scattering rate, a known result for electrons interacting with low-energy bosonic spin modes in *two* dimensions (see *e.g.*, [136]). Moving away from critical pressure, spin fluctuations decrease as shown on fig(17),

This corresponds to an intermediate situation where electrons scatter on both low and sizable energy modes. The former modes are still responsible for a linear term, though with a decreasing amplitude under pressure, while the latter modes favor the opening of a different scattering channel at high energy which fulfills the Fermi liquid requirements ($\omega_{sf} \gg T$). Scaling theory calculations confirm that as one moves away from the critical pressure, the scattering rate is no longer perfectly linear in temperature above T_c , but develops some curvature that is fitted quite satisfactorily by the $aT + bT^2$ form (see fig(10) of reference[103]).

3.4.2 Scattering and pairing, a common origin

Besides the seminal suggestion of Little for a non-phonon pairing mechanism in organics[18], several authors have made proposals for non-phonon pairing

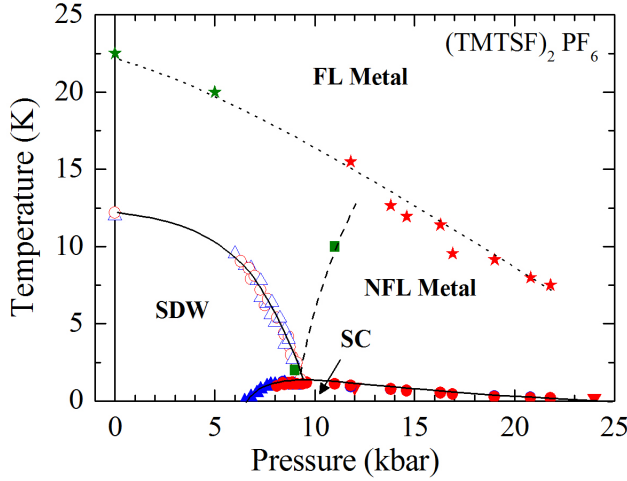


Fig. 17 Phase diagram of (TMTSF)₂PF₆ showing the limit T^* for the domain of dominant AF fluctuations (NFL metal) at the origin of the T linear resistivity (dotted line). The two stars data points above the *SDW* ground state are given by the temperature for the minimum of spin lattice $1/T_1$ relaxation [137]. In the FL metallic regime the temperature dependence of the resistivity is quadratic however high frequency optical conductivity data ($\omega \geq 1000\text{cm}^{-1}$) still provide a power law decay which is reminiscent of the Luttinger liquid behaviour[91,80,93]. The dashed line shows the pressure dependence of the AF fluctuations energy scale (Θ) derived from the temperature dependence of T_1T using the data from reference[137]. A similar behaviour for Θ versus P has been obtained by Bourbonnais and Sedeki[138] using data of (TMTSF)₂PF₆ under pressure published by Brown and Wu[125, 124]. Be aware of the ≈ 3 kbar difference between pressure scales of UCLA and Orsay for the phase diagram of (TMTSF)₂PF₆.

in inorganic metals. Let us emphasize some of the early works. In the context of the superconductivity in heavy fermions metals discovered the same year as organic superconductivity[139], J. Hirsch has performed a Monte Carlo simulation of the Hubbard model showing an enhancement of anisotropic singlet pairing correlations due to the on site Coulomb repulsion leading eventually to an anisotropic singlet superconducting state[140]. One year later, L. Caron and C. Bourbonnais[141,142] extending their theory for the generic (TM)₂X phase diagram to the metallic domain under pressure made the first proposal of a gap equation for singlet superconductivity based on an interchain magnetic coupling. While the need for an interchain pairing had been noticed early by V. Emery and coworkers (see [143] and [144,145]) the effective attraction in the gap equation of the Cooper channel is arising between carriers on neighbouring stacks as shown in the mean field renormalization theory[142,146]. This attraction is deriving from an interchain exchange interaction overcoming the on-stack Coulomb repulsion. However, the renormalization treatment of Q-1-D conductors has received more recently a significant improvement, taking into account the interference between the diverging Cooper and Peierls channels[147].

It is recognized that the weak-coupling limit explains fairly well the properties of the *SDW* phases in (TMTSF)₂X materials both the suppression of the *SDW* phase under pressure and the stabilization of magnetic field-induced *SDW* phases. The non interacting part of the quasi-one-dimensional electron gas model is defined in terms of a strongly anisotropic electron spectrum yielding an orthorhombic variant of the open Fermi surface in the $a-b$ plane of the Bechgaard salts. The spectrum $E(\mathbf{k}) = v_F(|k| - k_F) - 2t_\perp \cos k_\perp - 2t'_\perp \cos 2k_\perp$ as a function of the momentum $\mathbf{k} = (k, k_\perp)$ is characterized by an intrachain or longitudinal Fermi energy $E_F = v_F k_F$ which revolves around 3000 K in (TMTSF)₂X [62, 148]; here v_F and k_F are the longitudinal Fermi velocity and wave vector. This energy is much larger than the interchain hopping integral t_\perp (≈ 200 K), in turn much bigger than the second-nearest neighbor transverse hopping amplitude t'_\perp . The latter stands as the antinesting parameter of the spectrum which simulates the main influence of pressure in the model. The unnesting parameters of the band structure, t'_b and similarly t'_c for the c^* direction both play an important role in the $T - P$ and $T - P - H$ phase diagrams of (TMTSF)₂X.

First, when t'_b exceeds a critical unnesting band integral of the order of the *SDW* transition temperature ($\approx 15 - 30$ K in case of complete nesting[149, 150], the *SDW* ground state is suppressed in favour of a metallic phase with the possibility of restoration of spin density phases under magnetic field along c^* [151]. Second, the critical temperature for the stabilisation of the *SDW* subphases, $T_{FISDW}(H)$ should be steadily increasing from zero in a 2D conductor or in a fully nested 3D conductor in the "standard model"[152, 153]. However, since the real system is neither 2D nor perfectly nested ($t'_c > 0$), there exists a threshold field H_T for the appearance of *SDW* subphases defined by $T_{FISDW}(H_T) = t'_c$ [149]. Experimentally the threshold field is of the order of $2T$ [154, 155]

Second, within the framework of a weak-coupling limit the problem of the interplay between antiferromagnetism and superconductivity in the Bechgaard salts has been worked out using the renormalization group (RG) approach [127, 117] as sketched below taking into account only the 2D problem. The RG integration of high energy electronic degrees of freedom was carried out down to the Fermi level, and leads to a renormalization of the couplings at the temperature T [147, 156, 127]. The RG flow superimposes the $2k_F$ electron-hole (density-wave) and Cooper pairing many-body processes which combine and interfere at every order of perturbation. As a function of the 'pressure' parameter t'_\perp , a singularity in the scattering amplitudes signals an instability of the metallic state toward the formation of an ordered state at some characteristic temperature scale. At low t'_\perp , nesting is sufficiently strong to induce a *SDW* instability in the temperature range of experimental $T_{SDW} \sim 10 - 20$ K. When the antinesting parameter approaches the threshold t'^*_\perp from below ($t'^*_\perp \approx 25.4$ K, using the above parameters), T_{SDW} sharply decreases and as a result of interference, *SDW* correlations ensure Cooper pairing attraction in the superconducting d -wave (*SCd*) channel. This gives rise to an instability of the normal state for the onset of *SCd* order at the

temperature T_c with pairing coming from antiferromagnetic spin fluctuations between carriers of neighbouring chains. Such a pairing model is actually supporting the conjecture of interchain pairing in order for the electrons to avoid the Coulomb repulsion made by V. Emery in 1983 and 86[143,145].

The calculated phase diagram with reasonable parameters taking $g_1 = g_2/2 \approx 0.32$ for the backward and forward scattering amplitudes respectively and $g_3 \approx 0.02$ for the longitudinal Umklapp scattering term captures the essential features of the experimentally-determined phase diagram of $(\text{TMTSF})_2\text{PF}_6$ [127,138] to be compared with the experimental diagram on fig(17).

Third, Sedeki and Bourbonnais[157] have proceeded to an evaluation of the imaginary part of the one-particle self-energy. In addition to the regular Fermi-liquid component which goes as T^2 low frequency spin fluctuations yield $\tau^{-1} = aT\xi$, where a is constant and the antiferromagnetic correlation length $\xi(T)$ increases according to $\xi = c(T + \Theta)^{-1/2}$ as $T \rightarrow T_c$, where Θ is the temperature scale for spin fluctuations [157]. It is then natural to expect the Umklapp resistivity to contain (in the limit $T \ll \Theta$) a linear term AT besides the regular BT^2 , whose magnitude would presumably be correlated with T_c , as both scattering and pairing are caused by the same antiferromagnetic correlations. The observation of a T -linear law for the resistivity up to 8 K in $(\text{TMTSF})_2\text{PF}_6$ under a pressure of 11.8 kbar as displayed on fig(14) is therefore consistent with the value of $\Theta = 8\text{K}$ determined from NMR relaxation at 11 kbar on fig(13).

3.4.3 SDW conductive fluctuations very close to T_c

However, these recent studies of the low temperature regime were still unable to explain the very particular sublinear behaviour of the resistivity observed up to about three or four times T_c when the pressure is located in the very vicinity of the critical pressure P_c suppressing the insulating spin density wave (SDW) phase in $(\text{TMTSF})_2\text{PF}_6$ [129]. Therefore, in the vicinity of P_c , two precursor regimes can be distinguished, first the SC transition *per se* which is usually rather narrow in temperature, ($\Delta T \approx 0.1 - 0.2\text{K}$) and second, a broader temperature regime above T_c up to about 4K in which the sublinear resistivity is observed.

These two regimes have been reexamined using transport along the transverse c direction.

The major problem for the evaluation of an excess conduction coming from a collective motion independently of its exact origin is the proper determination of the temperature dependence of the background conduction due to the quasi particle scattering. Fortunately, such an investigation, carried out recently on $(\text{TMTSF})_2\text{PF}_6$ and $(\text{TMTSF})_2\text{ClO}_4$ and summarized in the previous Section has led to the determination of this background resistivity with a scattering rate behaving linearly in temperature (although not too close in temperature to T_c) and tightly connected to the value of T_c (which can be varied by pressure)[102,103].

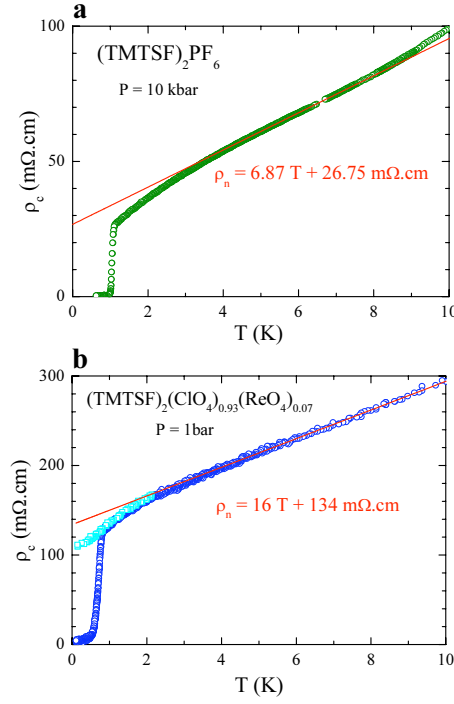


Fig. 18 Temperature dependence of ρ_c for $(\text{TMTSF})_2\text{PF}_6$ at a pressure close to 10 kbar, at zero field (a) and $(\text{TMTSF})_2(\text{ClO}_4)_{(1-x)}(\text{ReO}_4)_x$ $x = 7\%$ at ambient pressure at zero field and under a small magnetic field applied along c^* in order to suppress SC (b). The line is the linear fit for the normal state resistivity ρ_n between 4 and 8 K.

Two cases for the approach to superconductivity of $(\text{TMTSF})_2\text{X}$ are displayed in fig(18) when the compounds are located in their phase diagram close to the critical pressure for the stabilisation of SC . This pressure is real for $(\text{TMTSF})_2\text{PF}_6$ and amounts to 9.4 kbar[128,129]. In $(\text{TMTSF})_2\text{ClO}_4$, it is more likely a *virtual* negative pressure since SC is already stable under ambient pressure.

The first case shown on fig(18) is $(\text{TMTSF})_2\text{PF}_6$ under a pressure around 10 kbar. The second case refers to $(\text{TMTSF})_2\text{ClO}_4$ at ambient pressure in which T_c has been slightly depressed down to 0.75 K via the pair breaking of a controlled amount of non magnetic defects[100], see Sec (3.2).

We notice that in a material such as $(\text{TMTSF})_2\text{PF}_6$ where superconductivity arises in the neighborhood of a SDW ground state stable below the critical pressure P_c we can anticipate for the metallic phase above P_c a remnence of fluctuating SDW 's at low temperature. Actually, these low frequency AF fluctuations ($q = 2k_F$) are well known to contribute to the nuclear spin-lattice relaxation below 20 K or so[95]. Accordingly, they may be able to provide additional conductivity very much like incommensurate fluctuating CDW 's contribute in a low dimensional metal above the Peierls transition[33] given

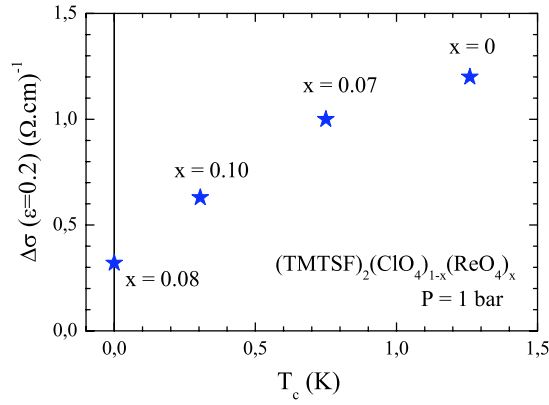


Fig. 19 Paraconductive contribution characterised by $\Delta\sigma$ ($\epsilon = (T - T_c)/T_c = 0.2$) (star symbols) in the precursor regime, versus T_c in the alloy series of $(\text{TMTSF})_2(\text{ClO}_4)_{1-x}(\text{ReO}_4)_x$ samples at 1 bar. The sample $x=0.1$ is superconducting whereas the one $x=0.08$, is not superconducting above 0.1 K although still displaying some fluctuating *SDW* conduction. This is nothing more than the indication that the nominal ReO_4 concentration is not the best way to characterize the amount of defects, at least for large concentrations.

the incommensurate character of the *SDW* firmly established by the observation of a double horn shape of the ^{13}C NMR spectrum in $(\text{TMTSF})_2\text{PF}_6$ [158]. The depression of the resistivity below 3 K is insensitive to the application of a magnetic field even up to 5 T *albeit* strongly suppressed by non magnetic defects. This feature enables to rule out any superconducting origin. It becomes then quite sensible to attribute it to the sliding of *SDW* fluctuations contributing to the paraconductivity $\Delta\sigma$. We can ascribe the drop of *SDW* paraconductivity displayed on fig(19) in doped samples to the net effect of pinning centers.

Substituting ReO_4 to ClO_4 amounts to a decrease of the mean distance between impurities. When the mean distance becomes comparable to the *SDW* coherence length, the impurity pinning suppresses $\Delta\sigma$ heavily [33]. Data for the *SDW* coherence length support this explanation since the zero-temperature longitudinal length ξ_{0a} is of order of 32 nm in $(\text{TMTSF})_2\text{PF}_6$ [159] *i.e.*, 44 times the distance between ClO_4 anions. Consequently, it is reasonable that the *SDW* is pinned by defects when the mean distance between pinning centers ≈ 7.3 nm (for 10% doping) is four times smaller than the coherence length leading in turn to a decrease of the fluctuation conduction independently of the current direction. The existence of a non perfect ClO_4 anion ordering in pure $(\text{TMTSF})_2\text{ClO}_4$ may also be the origin for a *SDW* paraconductivity contribution appearing to be smaller in $(\text{TMTSF})_2\text{ClO}_4$ than in $(\text{TMTSF})_2\text{PF}_6$.

4 Summarying, magnetism everywhere

(TMTSF)₂PF₆ - *Most remarkable electronic material ever discovered.* If Paul Chaikin says so on his personal Web site[160], it must be true because Paul is rarely wrong with his statements.

These superconductors are starting with materials where correlations and Umklapp scattering render the low dimensional electron system truly one dimensional as displayed by the 1D Mott localization on the left part of the generic diagram, fig(5). We may call this regime the strong coupling limit of the diagram. As pressure enhances the bare interstack coupling, 1D Mott localization is quickly suppressed when the Mott gap and the transverse coupling are of the same order. Then begins the weak coupling regime of the phase diagram with a Fermi surface whose nesting is responsible for the onset of a weak itinerant antiferromagnet at low temperature (the *SDW* state) leading in turn to an insulator since nesting of the Fermi surface is nearly perfect. Increasing the transverse coupling still further under pressure suppresses the *SDW* phase to the benefit of a metallic state becoming superconducting at low temperature.

However, superconductivity is not emerging from a Fermi liquid. NMR experiments reveal the existence of AF fluctuations dominant in the hyperfine $1/T_1$ at low temperature. Measurement of the spin susceptibility via relaxation data also reveal the 2D nature of these fluctuations. 2D AF fluctuations are actually governing the low temperature transport and the onset of superconductivity, both being tightly connected.

The weak coupling RG theory of the Q1D electron gas developed by Bourbonnais and his colleagues does reproduce very nicely most experimental features. Interestingly, they came to the conclusion that the two types of order are intimately connected namely, the non trivial result that antiferromagnetism and superconductivity love each other! Cooper pairing reinforces *SDW* correlations. AF fluctuations are also responsible for the linear- T resistivity which should increase as pressure approaches a magnetic quantum critical point. Actually the QCP is probably unaccessible for (TMTSF)₂PF₆ since it may correspond in terms of pressure to the zero temperature extrapolation of the *SDW* transition line. Hence P_{QCP} is likely to be smaller than P_c hidden inside the *SDW*/Metal(*SC*) coexistence regime[128,129], fig(20). A very detailed reinvestigation of the coexistence regime under pressure should be quite a worthwhile experimental program. For such a study helium gas would be a particularly well adapted pressure medium since this could allow a very fine control of the pressure without warming the whole pressure cell up to room temperature between each runs. Admittedly, the study of Seebeck and Nernst coefficient in (TMTSF)₂PF₆ under pressure should be very rewarding experiments[161]. For (TMTSF)₂ClO₄ the QCP is likely to be located at a negative pressure. This experiment is obviously impossible but an uniaxial elongation experiment has shown that an insulating ground state can be reacted in the relaxed state of (TMTSF)₂ClO₄ when some elongation is applied along the b direction[162] leading to a decrease of the b interchain coupling.

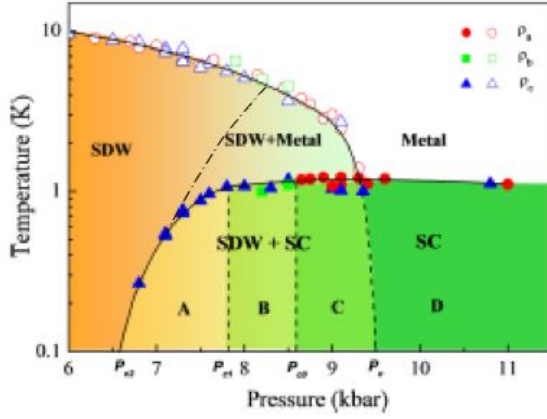


Fig. 20 Detailed determination of the phase diagram of $(\text{TMTSF})_2\text{PF}_6$ under zero magnetic field from resistivity measurements in the coexistence domain, according to refs[129, 128]. It is hard to tell where P_{QCP} could be located in this diagram but possibly in the region C of the figure.

When this coupling becomes smaller than the critical value stabilizing the metallic phase a *SDW* ground state is likely to be stabilized.

It is worth noting that the non Fermi liquid properties of the metallic background of Bechgaard salts prior to the onset of superconductivity may be quite a general behaviour when magnetism is close to superconductivity as noticed in reference[102]. For instance, the phase diagram of the iron-pnictide superconductors $\text{Ba}(\text{Fe}_{1-x}\text{Co}_x)_2\text{As}_2$, with its adjacent semi-metallic *SDW* and superconducting phases[163,164], presents a striking family resemblance with the diagram of $(\text{TM})_2\text{X}$. Comparison with the resistivity data of Fang *et al* [163] and Chu *et al* [164] on the pnictide superconductor $\text{Ba}(\text{Fe}_{1-x}\text{Co}_x)_2\text{As}_2$ suggests that the findings on $(\text{TMTSF})_2\text{PF}_6$ and $(\text{TMTSF})_2\text{ClO}_4$ may be a more general property of metals near a *SDW* instability. The phase diagram of $\text{Ba}(\text{Fe}_{1-x}\text{Co}_x)_2\text{As}_2$ [164,163], is similar to that of $(\text{TMTSF})_2\text{PF}_6$, with T_{SDW} and T_c both enhanced by a factor of about 20, and just above the critical doping where $T_{SDW} \rightarrow 0$ (at $x \approx 0.08$), its resistivity is purely linear below 125 K, down to at least $T_c \approx 25$ K, see fig(21). Furthermore, in the context of high- T_c cuprates, it has long been known that the low temperature resistivity of strongly-overdoped non-superconducting samples has the form $\rho(T) = \rho_0 + BT^2$, as in $\text{Tl}_2\text{Ba}_2\text{CuO}_{6+\delta}$ (Tl-2201) at $p = 0.27$ [165] and $\text{La}_{2-x}\text{Sr}_x\text{CuO}_4$ (LSCO) at $p = 0.33$ [166]. It was also shown that the evolution of $\rho(T)$ from $\rho(T) = \rho_0 + AT$ near optimal doping to $\rho(T) = \rho_0 + BT^2$ at high doping is best described by the approximate form $\rho(T) = \rho_0 + AT + BT^2$ at intermediate doping [167,168]. Recently, in a report of high-field resistivity data on overdoped LSCO [169], it was emphasized that the A coefficient thus obtained correlates with T_c , vanishing close to the point where superconductivity disappears.

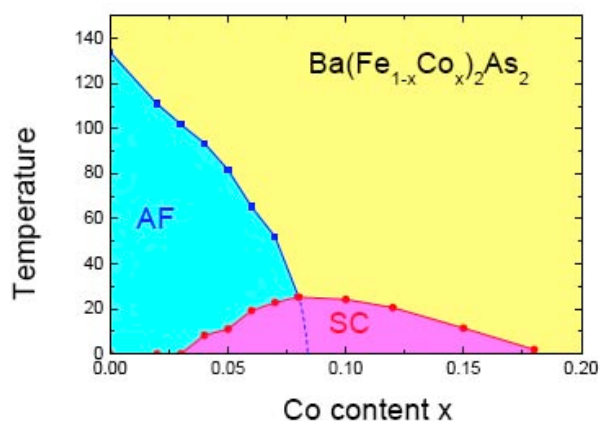


Fig. 21 Phase diagram of $\text{Ba}(\text{Fe}_{1-x}\text{Co}_x)_2\text{As}_2$ pnictides according to Fang et-al[163]. Notice the close resemblance with fig(17).

Electron-doped cuprates provide an other situation where a T linear resistivity and the proximity of an antiferromagnetic regime prevail in their phase diagram when Ce doping is varied. The resemblance between $\text{La}_{2-x}\text{Ce}_x\text{CuO}_4$ and $(\text{TMTSF})_2\text{PF}_6$ has been acknowledged recently[170] supporting earlier observation made on $\text{Pb}_{2-x}\text{Ce}_x\text{CuO}_4$ [171]. However, in the case of electron-doped cuprates there still remains some uncertainty regarding the exact location of the QCP in their phase diagram[170].

5 Conclusion and organic superconductivity in 2012

I have tried to show in this short presentation why the research on organic superconductors has been initiated and why it has started in the seventies in the context of a search for high temperature superconductivity boosted by two stimulating results.

First, a model suggested in 1964 by W. A. Little based on a phononless electron pairing leading to high T_c organic superconductivity. It is worth citing V.L.Ginzburg [172]: *I believe that it was undoubtedly the discussion of the possible exciton mechanism of superconductivity that stimulated the search for such superconductors and studies of them.* Ginzburg was thinking at the Little's proposal and the organic superconductors and intercalated layered superconductors which came later.

Second, the claim made by the Penn group in 1973 for precursor signs of a phonon-mediated superconductivity in the first organic conductor TTF-TCNQ just above the onset of a one dimensional metal insulator Peierls transition in TTF – TCNQ, the first organic metal.

The model of Little and the claims of the Penn group were probably overemphasized, but boosted the whole field at its start. The discovery of

superconductivity in the organic salt $(\text{TMTSF})_2\text{PF}_6$ in 1980 has shown how interesting this class of 1D organic conductors materials can be for the study of the physics of low dimensional conductors.

Research on organic superconductors has certainly been somehow overshadowed by the equally fascinating oxides and pnictides superconductors exhibiting superconductivity at much higher T_c but Ginzburg had quite a pragmatic approach to organics when he wrote again : *the organic superconductors are clearly interesting by themselves or, to be more precise, irrespective of the high T_c problem* .

High pressure has played a determining role for this discovery as often in the field of superconductors and governs the variety of phenomena which can be studied in a single sample keeping both the structure and the chemical purity constant. Furthermore, pressure is governing their physical properties, 1D Mott and Wigner localization and the wealth of various instabilities at low temperature which have shown how organic conductors compare fairly well in terms of scientific interest with the celebrated class of high T_c cuprates. In particular, the interplay between the Mott-driven localization of the 1D correlated electron gas and the 2D deconfinement under pressure is an issue central to the dimensionality crossover and also how the restoration of a Fermi liquid is achieved in quasi-one-dimensional conductor.

In such a brief account I could not go through the detailed physical properties of the Bechgaard and Fabre salts series of organic superconductors but the generic phase diagram that was gradually built over the years around these two series of compounds under either hydrostatic or chemical pressure stands out as a model of unity for the physics of low dimensional correlated systems. Much effort went to explain the multifaceted phase diagram of $(\text{TM})_2\text{X}$ as a whole, an attempt that also proved to be an active quest of unity for the theory.

At the starting point of the study of the Bechgaard salts more than thirty years ago, superconductivity was certainly one of the hardest part of the phase diagram to both explain and characterize. The mechanism of organic superconductivity in quasi-one-dimensional molecular crystals has been a related key issue in want of a satisfactory explanation for several decades. The statement of P.W. Anderson when he was interviewed a few years ago in a Physics Today issue dedicated to superconductivity, mentioning organic superconductors was: *These are still a complete mystery*. Hopefully, this has probably to be revised in the light of the recent experimental advances which confirm the non conventional nature of superconductivity in $(\text{TM})_2\text{X}$, as shown by the symmetry of the superconducting order parameter, as well as the issue of the presence and location of nodes for the gap which have now emerged from the experiments.

From a theoretical view point it is clear that electron correlations have walked in the superconducting pairing problem. The extensive experimental evidence in favor of the systematic emergence of superconductivity in $(\text{TM})_2\text{X}$ just below their stability threshold for antiferromagnetism has shown the need for a unified description of electronic excitations that lies at the core of both

density-wave and superconducting correlations. In this matter, the recent progresses achieved by the renormalization group method for the 1D-2D electron gas model have resulted in definite predictions about the possible symmetries of the superconducting order parameter when a purely electronic mechanism is involved, predictions that often differ from phenomenologically based approaches to superconductivity but are in fair agreement with the recent experimental findings. Although one can never be hundred percent sure at the moment, as far as recent results on 1D organic superconductivity are concerned magnetism and superconductivity cooperate.

What is emerging from the past work on these prototype 1D organic superconductors is their very simple electronic nature with only a single band at Fermi level, no prominent spin orbit coupling and extremely high chemical purity and stability. They should be considered in several respects as model systems to inspire the physics of the more complex high T_c superconductors, especially for pnictides and electron-doped cuprates. Most concepts discovered in these simple low dimensional conductors should be very useful for the study of other low dimensional systems such as carbon nanotubes or artificial 1D structures, *etc.*,.....The pairing mechanism behind organic superconductivity is likely different from the proposal made by Little but it is nevertheless a phonon-less mechanism, at least in $(\text{TM})_2\text{X}$ superconductors .

Of course, such a short overview is missing several of the very important aspects of the physics of 1D conductors namely, the magnetic field confinement discovered in the 1D's leading to the phenomenon of field induced spin density wave phases[173,174,175] and the quantization of the Hall effect in these phases[155,154,152]. Furthermore, the angular dependent magnetoresistance specific to these anisotropic conductors [86,176], (see [177] for a recent survey), the so-called Lebed-Osada-Danner-Chaikin oscillations in $(\text{TMTSF})_2\text{X}$ provide a nice illustration for the new features of the quasi-1D conductors[178].

Given the experimental constraints and difficulties tied to the use of extremely low temperature and high pressure conditions in $(\text{TM})_2\text{X}$, their properties will certainly continue to attract major experimental efforts in the next few years.

Let me tell the coming generation, *there is still plenty of food for thought in research on organic superconductivity!*

6 Acknowledgments

The search, discovery and study of organic superconductors has been a major research domain for the Solid State Physics Laboratory at Orsay over the last thirty years. We are all indebted to Professor Jacques Friedel for his contributions to this research at the Laboratoire de Physique des Solides.

I have been offered in 1967 by Jacques Friedel the creation of the group specialized in the study of metals and alloys under high pressure and low temperature. My first objective, the search for the excitonic instability in ytterbium under pressure and low temperature had not been a great success but

mastering high hydrostatic pressure experiments turned out to be a decisive asset for the investigation of periodic lattice distorted layer conductors and most definitely in the field of organic conductors and superconductors.

Professor Friedel has always supported and encouraged us with his wise advices and clever suggestions. This period has also been remarkably fruitful for the cooperation between chemists, theoreticians and experimentalists. I wish to address my sincere and deepest thanks to all my co-workers not only at Orsay but also at Sherbrooke (Québec), Copenhagen and Kyoto.

References

1. J. Bardeen, L.N. Cooper, and J.R. Schrieffer. *Phys. Rev.*, 108:1175, 1957.
2. H. Fröhlich. *Proc.Roy.Soc.A*, 223:296, 1954.
3. H.K. Onnes. *Proc. Akad. Wetenschappen*, 14:113, 1911.
4. G.F. Hardy and J.K. Hulm. *Phys.Rev.*, 93:1004, 1954.
5. J.Labbé and J.Friedel. *J.Physique*, 27:153, 1966.
6. M.Weger and I.R.Goldberg. in *Solid State Physics*, volume 28. Academic Press, New York, 1973.
7. J.Labbé, S.Barisić, and J.Friedel. *Phys.Rev.Lett*, 19:1039, 1967.
8. J Hulm and B. Matthias. *Science*, 208:881, 1980.
9. A. B. Migdal. *Sov.Phys.JETP.*, 7:996, 1958.
10. G. M. Eliashberg. *Sov.Phys.JETP.*, 11:696, 1960.
11. W. Kohn and J. M. Luttinger. *Phys. Rev. Lett.*, 15:524, 1965.
12. J. Friedel. *Adv in Physics*, 3:446, 1954.
13. J. Friedel. *Nuovo Cimento Suppl*, 2:287, 1958.
14. V.L.Ginzburg. *Jour.Experimental.Theoretical.Physics.(JETP)*, 47:2318, 1964.
15. V.L.Ginzburg. *Phys.Lett.*, 11:101, 1964.
16. A. W. Sleight, J. L. Gilson, and P. E. Bierstedt. *Solid. State. Comm*, 17:27, 1975.
17. A. A. Edelsack, D. U. Gubser, and S. A. Wolf. In S. A. Wolf and V. Z. Kresin, editors, *Novel Superconductivity*, page 1. Plenum Press, New Ork, 1987.
18. W.A. Little. *Phys. Rev. A*, 134:1416, 1964.
19. W.A. Little. *Scientific American*, 212:21, 1965.
20. H.N. McCoy and W.C. Moore. *J. Am. Chem. Soc.*, 33:273, 1911.
21. F. London. *Jour of Chemical Physics*, 5:837, 1937.
22. H. Akamatsu, H. Inokuchi, and Y. Matsunaga. *Nature*, 173:168, 1954.
23. W.A. Little. *J. Polymer. Sci C*, 29:17, 1970.
24. R.E. Peierls. in *Quantum Theory of Solids*. Oxford University Press, London, 1955.
25. R. Comès, M. Lambert, H. Launois, and H. R. Zeller. *Phys. Rev. B*, 8:571, 1973.
26. Yu. A Bychkov, L. P. Gorkov, and I.E. Dzyaloshinskii. *Sov. Phys. JETP*, 23:489, 1966.
27. F. Wudl, G.M. Smith, and E.J. Hufnagel. *J. Chem. Soc. Chem. Comm*, page 1453, 1970.
28. J. Ferraris, D.O. Cowan, W. Walatka, and J.H. Perlstein. *J. Am. Chem. Soc*, 95:948, 1973.
29. L.B. Coleman, M.J. Cohen, D.J. Sandman, F.G. Yamagishi, A.F. Garito, and A.J. Heeger. *Solid State Comm*, 12:1125, 1973.
30. G.A.Thomas *et al.* *Phys.Rev.*, B13:5105, 1976.
31. F. Denoyer, R. Comès, A.F. Garito, and A.H. Heeger. *Phys. Rev. Lett.*, 35:445, 1975.
32. R. H. Friend, M. Miljak, and D. Jérôme. *Phys. Rev. Lett.*, 40:1048, 1978.
33. D. Jérôme and H.J. Schulz. *Adv in Physics*, 31:299, 1982.
34. S. Yasuzuka, K. Murata, T. Arimoto, and R. Kato. *Jour. Phys. Soc. Japan*, 76:033701, 2007.
35. B. Horovitz, H. Gutfreund, and M. Weger. *Phys. Rev. B*, 12:3174, 1975.
36. J. P. Pouget, S. K. Khanna, F. Denoyer, R. Comès, A. F. Garito, and A. J. Heeger. *Phys. Rev. Lett.*, 37:437, 1976.
37. A.F. Garito and A.J. Heeger. *Accounts of Chemical Research*, 7:232, 1974.

38. E.M. Engler, B.A. Scott, S. Etemad, T. Penney, and V.V. Patel. *Jour. Am. Chem. Soc.*, 99:5909, 1977.
39. J.R. Andersen, K. Bechgaard, C.S. Jacobsen, G. Rindorf, H. Soling, and N. Thorup. *Acta Cryst.B.*, 34:1901, 1978.
40. C.S. Jacobsen, K. Mortensen, J.R. Andersen, and K. Bechgaard. *Phys. Rev. B*, 18:905, 1978.
41. Y. Tomkiewicz, J. R. Andersen, and A. R. Taranko. *Phys. Rev. B*, 17:1579, 1978.
42. J. P. Pouget. *Chemica Scripta*, 17:85, 1981.
43. A. Andrieux, P.M. Chaikin, C. Duroure, D. Jérôme, C. Weyl, K. Bechgaard, and J.R. Andersen. *J. Physique. Paris*, 40:1199, 1979.
44. J.L. Galigné, B. Liautard, S. Peytavin, G. Brun, , J.-M. Fabre, E. Torrelles, and L. Giral. *Acta Cryst.*, B 34:620, 1978.
45. K. Bechgaard, C.S. Jacobsen, K. Mortensen, H.J. Pedersen, and N. Thorup. *Solid.State.Comm*, 33:1119, 1979.
46. D. Jérôme, A. Mazaud, M. Ribault, and K. Bechgaard. *J. Phys. (Paris) Lett.*, 41:L95, 1980. Open archive on HAL <http://hal.archives-ouvertes.fr/>.
47. A. Andrieux, D. Jérôme, and K. Bechgaard. *J. Phys. Lett. Paris*, 42:L87, 1981. Open archive on HAL <http://hal.archives-ouvertes.fr/>.
48. W. M. Lomer. *Proc. Phys. Soc.*, 80:489, 1962.
49. A.W. Overhauser. *Phys. Rev*, 128:1437, 1962.
50. P. Molinié, D. Jérôme, and A. J. Grant. *Phil. Mag*, 30:1091, 1974.
51. J. A. Wilson, F. J. Di Salvo, and S. Mahajan. *Adv in Physics*, 24:117, 1975.
52. J. Friedel. *Jour. Physique.Lett*, 36:L 279, 1974. Open archive on HAL <http://hal.archives-ouvertes.fr/>.
53. D. Jérôme. *Science*, 252:1509, 1991.
54. H. Wilhelm, D. Jaccard, R. Duprat, C. Bourbonnais, D. Jérôme, J. Moser, C. Carcel, and J.M. Fabre. *Eur. Phys. Jour.*, B,21:175, 2001.
55. T. Adachi, E. Ojima, K. Kato, and H. Kobayashi. *Jour. Am. Chem. Soc.*, 122:3238, 2000.
56. P. Auban-Senzier, D. Jérôme, C. Carcel, and J.M Fabre. *J. Phy. IV France*, 114:41, 2004. Open archive on HAL <http://hal.archives-ouvertes.fr/>.
57. C. Bourbonnais and D. Jérôme. *Science*, 281:1156, 1998.
58. J. Friedel. *Jour. Physique. IV France*, 10 Pr3:3, 2000. Open archive <http://hal.archives-ouvertes.fr/>.
59. H. J. Schulz. *Phys. Rev. Lett.*, 64:2831, 1990.
60. J. Voit. *Rep. Prog. Phys.*, 58:977, 1995.
61. J. Solym. *Adv. Phys.*, 28:201, 1979.
62. L. Ducasse, A. Abderraba, J. Hoarau, M. Pesquer, B. Gallois, and J. Gaultier. *J. Phys. C*, 39:3805, 1986.
63. V. J. Emery, R. Bruinsma, and S. Barisic. *Phys. Rev. Lett.*, 48:1039, 1982.
64. T. Giamarchi. *Physica*, B230-232:975, 1997.
65. T. Giamarchi. *Quantum Physics in One-Dimension*. Clarendon Press, Oxford, 2004.
66. T. Giamarchi. *The Physics of Organic Superconductors and Conductors*, page 719. A. Lebed editor, Springer Verlag, Heidelberg, 2008.
67. M. Tsuchiizu, H. Yoshika, and Y. Suzumura. *Jour. Phys. Soc. Japan*, 70:1460, 2001.
68. C. Bourbonnais and L. G. Caron. *Int. J. Mod. Phys. B*, 5:1033, 1991.
69. C.Bourbonnais and D.Jérôme. *Advances in synthetic metals*. pages 206–261. Elsevier, New York, 1999.
70. S.Biermann, A.Georges, A.Lichtenstein, and T.Giamarchi. *Phys. Rev. Lett.*, 87:276405, 2001.
71. D.S. Chow, F. Zamborsky, B. Alavi, D.J. Tantillo, A. Baur, C.A. Merlić, and S.E. Brown. *Phys. Rev. Lett.*, 85:1698, 2000.
72. F. Nad, P. Monceau, C. Carcel, and J.M. Fabre. *Phys. Rev. B.*, 62:1753, 2000.
73. D.S. Chow, P. Wzietek, D. Foglatti, B. Alavi, D. J. Tantillo, C. A. Merlic, and S. E. Brown. *Phys. Rev. Lett.*, 81:3984, 1998.
74. L. Degiorgi and D. Jérôme. *Jour. Phys. Soc. Japan*, 75:051004, 2006.
75. K. Heuzé, M. Fourmigué, P. Batail, C. Coulon, R. Clérac, E. Canadell, P. Auban-Senzier, R. Ravy, and D. Jérôme. *Adv.Mater*, 15, 2003.

76. P. Auban-Senzier *et al.* *Phys. Rev. Lett.*, 102:255001, 2009.
77. N.F. Mott. *Metal-Insulator Transitions*. Taylor and Francis, London, 1974.
78. J. Moser, M. Gabay, P. Auban-Senzier, D. Jérôme, K. Bechgaard, and J. M. Fabre. *Eur. Phys. Jour. B*, 1:39, 1998.
79. A. Georges, T. Giamarchi, and N. Sandler. *Phys. Rev. B.*, 61:16393, 2000.
80. A. Pashkin, M. Dressel, and C. A. Kuntscher. *Phys. Rev.B.*, 74:165118, 2006.
81. C. Bourbonnais, F. Creuzet, D. Jérôme, K. Bechgaard, and A. Moradpour. *J. Phys. (Paris) Lett.*, 45:L755, 1984.
82. N. Cao T. Timusk and K. Bechgaard. *J. Physique (France)*, 6:1719, 1996. Open archive on HAL <http://hal.archives-ouvertes.fr/>.
83. A. Schwartz, M. Dressel, G. Grüner, V. Vescoli, L. Degiorgi, and T. Giamarchi. *Phys. Rev. B.*, 58:1261, 1998.
84. J. R. Cooper, L. Forró, B. Korin-Hamzić, K. Bechgaard, and A. Moradpour. *Phys. Rev. B*, 33:6810, 1986.
85. W. Kang, S. T. Hannahs, and P. M. Chaikin. *Phys. Rev. Lett.*, 69:2827, 1992.
86. T. Osada *et al.* *Phys. Rev. Lett.*, 66:1525, 1991.
87. G. M. Danner, W. Kang, and P. M. Chaikin. *Phys. Rev. Lett.*, 72:3714, 1994.
88. S. Sugawara *et al.* *J. Phys. Soc. Jpn.*, 75:053704, 2006.
89. W. Henderson *et al.* *Eur. Phys. Jour. B*, 11:365, 1999.
90. P. Auban-Senzier *et al.* *J. Phys. Cond. Matter*, 23:345702, 2011.
91. V. Vescoli, L. Degiorgi, W. Henderson, G. Grüner, K. P. Starkey, and L.K. Montgomery. *Science*, 281:1181, 1998.
92. F. Zwick *et al.* *Solid. State. Comm.*, 113:179, 2000.
93. A. Pashkin, M. Dressel, and M. Handfland C. A. Kuntscher. *Phys. Rev.B*, 81:125109, 2010.
94. F. Creuzet, C.Bourbonnais, L.G. Caron, D. Jérôme, and K. Bechgaard. *Synthetic Metals*, 19:289, 1987.
95. C.Bourbonnais and D.Jérôme. *The Physics of Organic Superconductors and Conductors*, page 357. A. Lebed editor, Springer Verlag, Heidelberg, 2008.
96. M. Takigawa and G. Saito. *J. Phys. Soc. Jpn.*, 55:1233, 1986.
97. I. J. Lee, S. E. Brown, W. Yu, M. J. Naughton, and P. M. Chaikin. *Phys. Rev. Lett.*, 94:197001, 2005.
98. S. Belin and K. Behnia. *Phys. Rev. Lett.*, 79:2125, 1997.
99. J. Shinagawa, Y. Kurosaki, F. Zhang, C. Parker, S. E. Brown, and D. Jérôme. *Phys.Rev.Lett.*, 98:147002, 2007.
100. N.Joo, P. Auban-Senzier, C. Pasquier, D.Jérôme, and K. Bechgaard. *Eur.Phys.Lett*, 72:645, 2005.
101. S. Yonezawa, Y. Maeno, K. Bechgaard, and D. Jérôme. arxiv.org/abs/1112.5974, (to be published, 2012).
102. N. Doiron-Leyraud, P. Auban-Senzier, S. René de Cotret, C. Bourbonnais, D. Jérôme, K. Bechgaard, and L. Taillefer. *Phys. Rev. B*, 80:214531, 2009.
103. N. Doiron-Leyraud, P. Auban-Senzier, S. René de Cotret, C. Bourbonnais, D. Jérôme, K. Bechgaard, and L. Taillefer. *Eur. Phys. Jour.B*, 78:23, 2010. DOI 10.1140/epjb/e2010-10571-4.
104. I. J. Lee, M. J. Naughton, G. M. Danner, and P. M. Chaikin. *Phys. Rev. Lett.*, 78:3555, 1997.
105. I. J. Lee, S. E. Brown, W. G. Clark, M. J. Strouse, M. J. Naughton, W. Kang, and P.M. Chaikin. *Phys.Rev.Lett.*, 88:017004, 2001.
106. H. Shimahara. *Jour. Phys. Soc. Japan*, 69:1966, 2000.
107. N. Belmechri, G. Abramovici, M. Héritier, S. Haddad, and S. Charfi-Kaddour. *Eur. Phys. Lett*, 80:37004, 2007.
108. P. Fulde and R. A. Ferrell. *Phys. Rev.*, 135:A550, 1964.
109. A. I. Larkin and Y. N. Ovchinnikov. *Sov. Phys. JETP.*, 20:762, 1965.
110. J.P. Pouget. in *Low Dimensional Conductors and Superconductors*. D. Jérôme and L.G. Caron editors, Plenum Press, New York, 1987.
111. S. Tomić, D. Jérôme, D. Mailly, M. Ribault, and K. Bechgaard. *J. Physique*, 44 C3:1075, 1983. Open archive <http://hal.archives-ouvertes.fr/>.
112. S. Tomić, D. Jérôme, P. Monod, and K. Bechgaard. *J. Physique*, 44-C3:1346, 1983. Open archive <http://hal.archives-ouvertes.fr/>.

113. P. Garoche, R. Brusetti, and K. Bechgaard. *Phys. Rev. Lett.*, 49:1346, 1982.
114. S. Ravy, R. Moret, J. P. Pouget, and R. Comès. *Physica*, 143 B:542, 1986.
115. L.P. Gorkov and D. Jérôme. *J. Phys. Lett.*, 46:L-643, 1985. Open archive on HAL <http://hal.archives-ouvertes.fr/>.
116. K. Maki, H. Won, and S. Haas. *Phys. Rev. B*, 69:012502, 2004.
117. J. C. Nickel, R. Duprat, C. Bourbonnais, and N. Dupuis. *Phys. Rev. Lett.*, 95:247001, 2005.
118. G. E. Volovik. *JETP Lett*, 58:469, 0993.
119. M. Yamashita *et al.* *Phys. Rev. B*, 84:060507, 2011.
120. T. Sakakibara *et al.* *J. Phys. Soc. Japan*, 76:051004, 2007.
121. A. G. Lebed and S. Wu. *Phys. Rev. B*, 82:172504, 2010.
122. H.J. Schulz, D. Jérôme, M. Ribault, A. Mazaud, and K. Bechgaard. *J. Physique. Lett*, 42:L-51, 1981. Open archive on HAL <http://hal.archives-ouvertes.fr/>.
123. K. Bechgaard, K. Carneiro, M. Olsen, and F. B. Rasmussen. *Phys. Rev. Lett*, 46:852, 1981.
124. S. E. Brown *et al.* In A. Lebed, editor, *The Physics of Organic Superconductors and Conductors*, page 76, Heidelberg, 2008. Springer Series in Materials Sciences.
125. W. Wu *et al.* *Phys. Rev. Lett*, 94:097004, 2005.
126. T. Moriya. *Adv. Phys.*, 49:555, 2000.
127. C. Bourbonnais and A. Sedeki. *Phys. Rev. B*, 80:085105, 2009.
128. T. Vuletić, P. Auban-Senzier, C. Pasquier, S. Tomić, D. Jérôme, M. Héritier, and K. Bechgaard. *Eur. Phys. Jour. B*, 25:319, 2002.
129. N. Kang *et al.* *Phys. Rev. B*, 81:100509, 2010. cond-mat:1002.3767v1.
130. M. Ribault, G. Benedek, D. Jérôme, and K. Bechgaard. *J. Phys. Lett. Paris*, 41:L-397, 1980.
131. S. Yonezawa, Y. Maeno, P. Auban-Senzier, C. Pasquier, K. Bechgaard, and D. Jérôme. *Phys. Rev. Lett.*, 100:117002, 2008.
132. S.S.P. Parkin *et al.* *Mol. Cryst. Liq. Cryst*, 1985.
133. K. Kadowaki and S. B. Woods. *Solid. State. Comm*, 58:507, 1986.
134. J. P. Pouget, S. Kagoshima, T. Tamegai, Y. Nogami, K. Kubo, T. Nakajima, and K. Bechgaard. *J. Phys. Soc. Japan*, 59:2036, 1990.
135. N. Doiron-Leyraud *et al.* *Phys. Rev. B*, 80:214531, 2009.
136. A. Abanov *et al.* *Adv. Physics*, 52:119, 2003.
137. F. Creuzet, D. Jérôme, and A. Moradpour. *Mol. Cryst. Liq. Cryst.*, 119:297, 1985.
138. C. Bourbonnais and A. Sedeki. *Comptes Rendus Physique*, 12:532, 2011.
139. F. Steglich, J. Aarts, W. Lieke C.D. Bredl, D. Meschede, W. Franz, and H. Schäfer. *Phys. Rev. Lett.*, 43:1892, 1979.
140. J.E. Hirsch. *Phys. Rev. Lett.*, 54:1317, 1985.
141. C. Bourbonnais and L. G. Caron. *Physica*, 143B:450, 1986.
142. L. G. Caron and C. Bourbonnais. *Physica*, 143B:453, 1986.
143. V. J. Emery. *J. Physique*, 44-C3:977, 1983. Open archive <http://hal.archives-ouvertes.fr/>.
144. M.T. Béal-Monod, C. Bourbonnais, and V. J. Emery. *Phys. Rev. B*, 34:7716, 1986.
145. V. J. Emery. *Synthetic. Met*, 13:21, 1986.
146. C. Bourbonnais and L.G. Caron. *Europhys. Lett.*, 5:209, 1988.
147. R. Duprat and C. Bourbonnais. *Eur. Phys. J. B*, 21:219, 2001.
148. D. Lepevelen *et al.* *Eur. Phys. J. B*, 19:363, 2001.
149. G. Montambaux. In D. Jérôme and L. G. Caron, editors, *Low-Dimensional Conductors and Superconductors*, page 233, New York, 1987. Plenum Press.
150. T. Ishiguro, K. Yamaji, and G. Saito. *Organic Superconductors*. Springer Verlag, Berlin-Heidelberg, 1998.
151. T. Ishiguro, K. Yamaji, and G. Saito. *Organic Superconductors*. Springer, Berlin, 1998.
152. M. Héritier, G. Montambaux, and P. Lederer. *J. Phys. (Paris) Lett.*, 45:L943, 1984.
153. M. Héritier. In D. Jérôme and L. G. Caron, editors, *Low-Dimensional Conductors and Superconductors*, page 243, New York, 1987. Plenum Press.
154. S.T. Hannahs, J.S. Brooks, W. Kang, L.Y. Chiang, and P.M. Chaikin. *Phys. Rev. Lett.*, 63:1988, 1989.

-
155. J.R. Cooper, W. Kang, P. Auban, G. Montambaux, D.J  rome, and K. Bechgaard. *Phys.Rev.Lett.*, 65:1984, 1989.
156. J. C. Nickel, R. Duprat, C. Bourbonnais, and N. Dupuis. *Phys. Rev. B*, 73:165126, 2006.
157. A. Sedeki, D. Bergeron, and C. Bourbonnais. *Physica B*, 405:89, 2010.
158. E. Barthel, G. Quirion, P. Wzietek, and D.J  rome. *Europhys. Lett.*, 21:87, 1993.
159. G. Gr  ner. *Rev. Mod. Phys.*, 66:1, 1994.
160. P. M. Chaikin. <http://www.physics.nyu.edu/~pc86/organics.html>.
161. K. S. Kim and C. P  pin. *Phys. Rev. B*, 83:073104, 2011.
162. H. Kowada, R. Kondo, and S. Kagoshima. *Jour. Phys. Soc. Japan*, 11:114710, 2007.
163. L.Fang *et al.* *Phys. Rev. B*, 80:140508(R), 2009. arXiv.org:0903.2418.
164. J. H. Chu *et al.* *Phys. Rev. B*, 79:014506–1, 2009.
165. T. Manako *et al.* *Phys. Rev. B*, 46:11019, 1992.
166. S. Nakamae *et al.* *Phys. Rev. B*, 68:100502, 2003.
167. A. P. Mackenzie *et al.* *Phys. Rev. B*, 53:5848, 1996.
168. C. Proust *et al.* *Phys. Rev. Lett.*, 89:147003, 2003.
169. R. A. Cooper *et al.* *Science*, 323:603, 2009.
170. K. Jin *et al.* *Nature*, 476:73, 2011.
171. P. Fournier *et al.* *Phys. Rev. Lett.*, 81:4720, 1998.
172. V.L. Ginzburg. *Progress in Low Temperature Physics*, 12:1, 1989.
173. M. Ribault, D. J  rome, J. Tuchendler, C. Weyl, and K. Bechgaard. *J. Phys. Lett.*, 44:L–953, 1983. Open archive on HAL <http://hal.archives-ouvertes.fr/>.
174. P. M. Chaikin, Mu-Yong Choi, J. F. Kwak, J. S. Brooks, K. P. Martin, M. J. Naughton, E. M. Engler, and R. L. Greene. *Phys.Rev.Lett.*, 51:2333, 1983.
175. L. P. Gorkov and A. G. Lebed. *J. Phys. (Paris) Lett.*, 45:L433, 1984. Open archive on HAL <http://hal.archives-ouvertes.fr/>.
176. M. J. Naughton, O. H. Chung, M. Chaparala, X. Bu, and P. Coppens. *Phys.Rev.Lett.*, 67:3712, 1991.
177. T. Osada and E. Ohmichi. *Jour. Phys. Soc. Japan*, 75:051006, 2006.
178. A.G. Lebed. *Sov. Phys. JETP. Lett*, 43:174, 1986.